

Review

Construction of intelligent moving micro/nanomotors and their applications in biosensing and disease treatment

Yingshu Guo^{1†✉}, Dan Jing^{1†}, Shiwei Liu¹, and Quan Yuan^{2✉}

1. Shandong Provincial Key Laboratory of Molecular Engineering, School of Chemistry and Chemical Engineering, Qilu University of Technology (Shandong Academy of Sciences), Jinan 250353, P. R. China.
2. Molecular Science and Biomedicine Laboratory, State Key Laboratory of Chemo/Biosensing and Chemometrics, College of Chemistry and Chemical Engineering, Hunan University, Hunan University, Changsha, 410082, P. R. China.

† Yingshu Guo and Dan Jing contributed equally to this work.

✉ Corresponding authors: yingshug@126.com (Y. Guo); yuanquan@whu.edu.cn. (Q. Yuan).

© The author(s). This is an open access article distributed under the terms of the Creative Commons Attribution License (<https://creativecommons.org/licenses/by/4.0/>). See <http://ivyspring.com/terms> for full terms and conditions.

Received: 2022.12.14; Accepted: 2023.04.26; Published: 2023.05.15

Abstract

Micro/nanomotors are containers that pass through liquid media and carry cargo. Because they are tiny, micro/nanomotors exhibit excellent potential for biosensing and disease treatment applications. However, their size also makes overcoming random Brownian forces very challenging for micro/nanomotors moving on targets. Additionally, to achieve desired practical applications, the expensive materials, short lifetimes, poor biocompatibility, complex preparation methods, and side effects of micro/nanomotors must be addressed, and potential adverse effects must be evaluated both *in vivo* and in practical applications. This has led to the continuous development of key materials for driving micro/nanomotors. In this work, we review the working principles of micro/nanomotors. Metallic and nonmetallic nanocomplexes, enzymes, and living cells are explored as key materials for driving micro/nanomotors. We also consider the effects of exogenous stimulations and endogenous substance conditions on micro/nanomotor motions. The discussion focuses on micro/nanomotor applications in biosensing, treating cancer and gynecological diseases, and assisted fertilization. By addressing micro/nanomotor shortcomings, we propose directions for further developing and applying micro/nanomotors.

Keywords: micro/nanomotor, biosensing, disease treatment, targeted movement

1. Introduction

Power units are the most distinctive features essential to the structure and operation of micro/nanomotors, which are frequently delivered through the bloodstream to target organs or tissues when employed *in vivo* for biosensing or treating diseases. Owing to their extremely small size (and mass), micro/nanomotors undergo severe shear stress in the bloodstream, which increases their rotational velocity and may lower their therapeutic efficacy. To solve this problem, these negative impacts can be mitigated if a motor unit is installed. Thus, targeted drug delivery can be powered by micro/nanomotors to overcome

blood-flow resistance [1] and achieve efficient and rapid localization.

In 2002, Whitesides *et al.* developed a chemical-fuel-powered self-propelled plate. Since then, several important advances have been made in the study, generation, and development of micro/nanomotors [2]. Nanoparticles (NPs) and their materials have many applications, including the containment and delivery of medicinal products, such as small molecules, biologics, and nucleic acids [3]. Recently, micro/nanomotors have enabled various conceivable microoperations and typically comprise fluid-

moving, multifunctional nanostructures constructed based on different materials and shapes [4]. Recently, research has been continued on the essential elements and circumstances that regulate power in micro/nanomotors. For example, metallic nanomaterials [5], enzymes [6], living cells [7], compound nanomaterials [8], and composite nanomaterials [9,10] can drive micro/nanomotors. Additionally, many natural molecular machines, such as DNA and proteins [11], and many plants exhibit natural drug-carrying structures and simple and effective self-motion mechanisms, which can be combined with other key materials to develop environmental and biomedical applications [12].

An essential component of next-generation drug loading is self-driving carriers that can transport drugs to targets based on specified biomarkers. Such carriers use self-propelled micro/nanomotors and pumps. However, some metals used in self-propelled systems are poisonous to healthy cells and cannot be degraded. Therefore, scientists have developed various micro/nanomotor-driving media. The micro/nanomotor size, favorable biocompatibility [13], orientation and targeting prowess [14], and drug loading have made such motors useful for various applications [15], such as biosensing [16-19] and treating diseases [20-23].

Owing to a wider application range, micro/nanomotor usage has recently become more diversified. Herein, we discuss nanomotors in depth in relation to their key materials and external stimuli, such as light [24-27]; magnetism [28-30]; sound [31, 32]; electricity [33]; and endogenous substances, including water [34], urea [35], glucose [36], hydrogen peroxide [37, 38], and gastric acid protons [39-41]. The

applications of micro/nanomotors in biosensing and treating diseases are discussed in detail, and directions for further research and application prospects of micro/nanomotors are outlined in **Figure 1**.

2. Key materials for developing micro/nanomotors

2.1. Metallic nanocomplexes

For conventional rockets, the Reynolds number is 10^6 ; however, for microrockets, it is just 10^{-4} , which is very low. This means that inertia negligibly affects the rocket movement, and instantaneous force usually translates to instantaneous movement. In other words, to move a microrocket continuously in the human body, a continuous driving force must be provided. In addition, for micromotions, the considerable impact of the Brownian motion cannot be ignored. Consequently, the provision of a stable and sustainable propulsion force is the first challenge that researchers have encountered when constructing microrockets [42].

Often, asymmetric product distribution (including gases), which is generated by the redox reaction of the fuel that powers device bodies, functions as the propelling principle for chemically propelled micro/nanorobots. Following the loading of the catalyst onto the micro/nanomotor, redox reactions between the catalyst and fuel produce bubbles. As the bubbles break from the robot body, they generate motion by generating momentum in the opposite direction. An essential component of a bubble-driven tubular micro/nanomotor's overall motion is the bubbles' dynamic evolution. Owing to their rapid

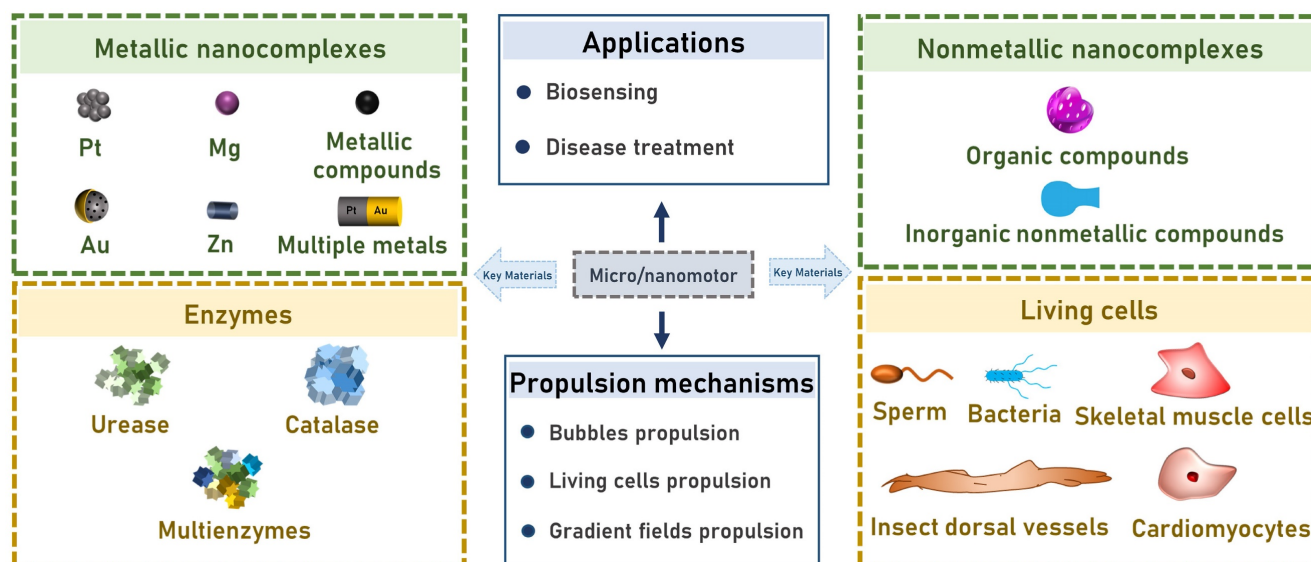


Figure 1. A summary of the classification and applications for biosensing and disease treatment of micro/nanomotors.

velocity and enormous power, such micro/nanomotors have garnered considerable research interest. To catalyze the production of gas from endogenous substances in living tissues or cells, metal NPs have been used as a crucial component of the driving force behind molecular motors. The most typical propulsion mechanisms for micro/nanomotors catalyzed by metals or metal oxides may be bubble propulsion or self-diffusiophoresis. When a metal catalyzes the oxidation of hydrogen peroxide, oxygen is produced by a redox reaction, and the micro/nanomotor advances because of a gradient in the O₂ concentration. Finite element analysis can be used to model such gradients [43, 44]. The inversion symmetry is broken by the Brownian ratchet diffusion mechanism. Without relying on the thermodynamic equilibrium, the directional motion is conceivable in the context of a Brownian ratchet. The developed DNA origami functions as a spinning nanomotor with a ratchet-based driving mechanism [45]. The primary materials used for propelling micro/nanomotors and a summary of recent research are listed in **Table 1**.

2.1.1 Pt

A typical micro/nanomotor can be constructed from an inert microsphere semicoated with Pt to accelerate H₂O₂ decomposition. The Pt asymmetry decomposes hydrogen peroxide to produce oxygen, which is then used by the Pt catalytic activity to power the micro/nanomotor. Then, Pt is changed asymmetrically through the micro/nanomotor, which is powered by the photothermal conversion.

Hwang *et al.* used asymmetric Pt modification to develop a micro/nanomotor that could remove Cs ions from water by functionalizing silica microspheres with CuFC, depositing magnetic nickel on half of the microsphere surfaces and a Pt catalyst layer on the other half. The Pt on the microsphere surfaces decomposed hydrogen peroxide in the solution, which formed bubbles on the microsphere surfaces and accelerated the micromotion. The metallic Ni layer enabled the micro/nanomotor to be regulated remotely while considerably accelerating the propulsion by stimulating an external magnetic field [46]. A similar micro/nanomotor was developed by Díez *et al.* [14] using metallic Pt for asymmetrically changing the surface of mesoporous materials. The mesoporous silica NP (MSNP) face functioned as a drug-loaded nanocontainer, the platinum nanodendrite face functioned as the driving element, and the disulfide-containing oligo (ethylene glycol) chain (S-S-PEG) functioned as the gating mechanism. The nanomotor accelerated the self-propulsion of bubbles by catalyzing the decomposition of low-concentration hydrogen peroxide to turn chemical energy into

oxygen. Another team varied the motion of a deformed Pt-PAzoMA Janus micromotor (JM) (**Figure 2A**) comprising homopolymer poly[6-(4-methoxy-4'-oxyazobenzene) hexyl methacrylate] (PAzoMA) particles, wherein half of the particle surfaces were coated with Pt [47]. The motion was inspired by the natural landing of flying squirrels. When hydrogen peroxide was employed as fuel, a considerable oxygen gradient was generated on the Pt side of the particles, indicating that self-diffusion electrophoresis functioned based on the propulsion principle. Using the same theory, Chan Woo Park *et al.* asymmetrically deposited metallic Pt to fabricate micro/nanomotors [48]. Half of the Pt NPs were deposited on the surface of magnetic illite microspheres so that Pt catalyzed the decomposition of hydrogen peroxide to generate asymmetric bubbles and achieve self-propulsion. The micro/nanomotor exhibited a high velocity of 265 μm/s. In addition, Yeonsoo Lee *et al.* used a self-propelled micro/nanomotor for selectively removing cesium from a high-salt environment by generating asymmetric bubbles through the Pt-catalyzed decomposition of hydrogen peroxide [49].

First, the micro/nanomotor added sulfur to NaX to improve Cs⁺ selectivity by increasing additional Lewis acid-base interactions and then half-deposited on Pt on the S-NaX surface, which catalytically decomposed H₂O₂ to push the bubbles. In addition to catalyzing endogenous chemicals, Pt can perform photothermal conversion, which helps nanomotor propulsion. Wan *et al.* produced a mesoporous/macroporous silica (MMS)/platinum (Pt) nanomotors coated with a platelet membrane [50]. Owing to the nonuniform distribution of Pt NPs in the system, when the micro/nanomotor was externally stimulated using a near-infrared (NIR) light, the motor generated heat unevenly. Therefore, thermophoresis was the nanomotor driving force [51].

2.1.2 Mg

Hydrogen peroxide, which is hazardous to living tissues and cells, can potentially be replaced by water, which is ubiquitous in organisms and, therefore, may be a perfect energy source. Mg is an active metal that combines with water and H⁺ to produce gas. Several Mg-based micro/nanomotors have been examined and explored by various researchers.

Exploiting the Mg activity, Emil Karshalev *et al.* designed an Mg-based micro/nanomotor oral pill by uniformly dispersing Mg-based micro/nanomotors in a pill matrix [40]. A Mg/TiO₂ poly(lactic-co-glycolic acid) (Mg/TiO₂/PLGA) micro/nanomotor carried the cargo. When the pills reached the strongly acidic gastric environment, they were activated, and gastric juices rapidly decomposed and dissolved the sugar

matrix, which released the pill's contents. The engine's magnesium core reacted with the stomach acid to produce hydrogen gas, which produced efficient bubble propulsion. Using the same catalytic decomposition mechanism, Zhang *et al.* combined a Mg-based micro/nanomotor with living macrophage (MΦ) cells to form a unique MΦ-Mg biohybrid motor system [52]. When the motor was placed in an acidic environment, the Mg core chemically reacted with protons in the acidic liquid, and the motor generated hydrogen tail bubbles, which provided propulsion. Additionally, Mg is an active metal that can use water as a fuel source and reacts to generate hydrogen and self-propulsion. Wang *et al.* proposed a method for sequentially modifying PLGA, sodium alginate (ALG), chitosan (CHI), and anti-CD3 on the upper surface of Mg microspheres to fabricate anti-CD3-loaded PLGA/ALG/CHI Mg micro/nanomotor systems [53] exhibiting degradable components that were self-propelled by the reaction between Mg and

water to generate gas so that the micro/nanomotors exhibited good biological properties and compatibility. Similarly, researchers have produced organic-inorganic hybrid Mg micro/nanomotors for enhanced catalytic activity and synergistic hydrogen chemotherapy [54]. Biodegradable micro/nanomotors were prepared utilizing Mg microparticle templates and then asymmetrically coated with PLGA. Magnesium reacted with water to generate enough H₂ to drive the micro/nanomotor motion and enable enhanced diffusion.

2.1.3 Zn

In addition to Pt and Mg micro/nanomotors, Zn-based ones are frequently used as propellers. The entire motion of bubble-driven tubular micro/nanomotors critically depends on the bubbles' dynamic behavior. Because of their rapid velocity and high power, bubble-driven micro/nanomotors exhibit considerable responsiveness.

Table 1. A summary of the properties of micro/nanomotors according to the key materials driving them.

Key material	Particle size	Motion speed	Movement mechanism	Application	Advantage	Ref.	
Metallic nanocomplexes	Pt	~20.28 ± 7.55 μm	265.52 ± 41.85 μm/s	Bubbles propulsion	Improved the Cs adsorption	[48]	
	Mg	10-25 μm (D)	~127.3 μm/s	Bubbles propulsion	Fulfill diverse biological tasks	[52]	
	Zn	8.9 ± 0.7 μm (D)	203.5 μm/s	Bubbles propulsion	Target treatment of bacterial infections	[59]	
	Au	67.8-80.6 nm (D)	~1.46-6.44 μm/s	Self-thermophoretic force	Recognizing cancer cells	[60]	
	Metallic compounds (MnO ₂)	~2 μm (ID) ~5 μm (D) ~10 μm (L)	77.2-466.4 μm/s	Bubbles propulsion	—	Low cost, wide fuel concentration range, easiness of fabrication, tunable crystal structure and surface morphology, controllable size and geometry, high efficiency and long lifespan.	[10]
Nonmetallic nanocomplexes	Multiple metals (Au/Pt)	62 ± 3 nm (D)	20.4 μm/s	Concentration gradient	Drug-molecule cargo loading	The motion-behavior endowed efficient cellular uptake of micro/nanomotors.	[72]
	Inorganic nonmetallic compounds	4.0 mm (D) 6.0 mm (L)	14.78 ± 4.82 mm/s	Bubbles propulsion	Targeted bactericidal effect	—	[80]
	Organic compounds (HLA _n)	~120-385 nm (D)	3-13 μm/s	Bubbles propulsion	Promoting revascularization and anti-tumor	Zero-waste and self-destroyed nanomotors.	[85]
Enzymes	Urease	—	~4.04 μm/s	Concentration gradient	—	—	[101]
	Catalase	13.5 μm (L) ~3.0 μm (ID)	420 ± 18 μm/s.	Bubbles propulsion	Detect a variety of biomolecules	Good selectivity and reproducibility, excellent stability and assay performance.	[102]
	Multi-enzymes	41 ± 2 nm (D)	—	Bubbles propulsion	—	Synergistically promote the efficacy of the enzyme-driven nanomotor, NIR light-triggered PDT and GOx-induced ST effects.	[110]
Living cells	Sperm	> 50 μm (L) ~ 5 μm (D)	76 ± 17 μm/s	The sperm flagellum	Magnetic guidance and cargo transport	Strong sperm propulsion, sperm rheotaxis, biocompatibility	[123]
	Bacteria (Escherichia coli bacterium)	—	22.5 μm/s	Bacteria-driven	Drug delivery	The bacteria can be integrated with synthetic substances to produce multiple functionalities through their biological actuation and sensing capabilities.	[125]
	Cardiomyocytes	~ 100 μm (THK)	—	Cardiomyocyte beating	—	—	[135]
	Insect dorsal vessels	150 μm (D)	3.5 μm/s	Insect dorsal vessel tissue contracting	—	Contracting autonomously and more environmentally.	[138]
	Skeletal muscle cells	0.5-11.7 μm (THK)	—	Skeletal myotubes	Biohybrid devices with predictable functionality	—	[143]

With Zn as the key material, micro/nanomotors are propelled by generating air bubbles. Zhou *et al.* used poly(amino acid) to develop a drug-loaded microrocket [55] comprising a Zn-particle core, a thin iron (Fe) middle layer, and a poly(aspartic acid) outer layer. The microrocket was magnetically controlled by adding an iron layer. Owing to its good compatibility and safety, iron has been widely applied as a biomedical material [56]. When the microrocket was immersed in a gastric acid simulant, numerous hydrogen bubbles were released and generated self-propulsion. Using the same mechanism, researchers designed a multichambered tubular micro/nanomotor with a cargo compartment protected by a pH-responsive cap at the front end and a zinc motor at the back end to achieve a site-specific response to cargo release and prolong retention in gastric tissue [57]. This micro/nanomotor exhibited a powerful push in gastric acid. In an acidic environment, zinc reacted with gastric acid protons, which enabled rapid and autonomous directional actuation. Recently, Cui *et al.* designed a microrod comprising a zinc core and positively charged poly(3,4-ethylenedioxythiophene) (PEDOT⁺) shell containing an anionic model drug dissolved in an electrolyte solution [58]. A galvanic cell was formed to construct a battery-operated drug delivery system. When the zinc-based microrod battery was immersed in a physiological environment at a certain pH, both groups of redox reactions proceeded spontaneously, and the reaction progression depended on the pH of the immersion environment. At low pH levels, H⁺ was converted to H₂, and bubble generation produced a recoil force on the microrod, which caused the micro/nanomotor to operate autonomously. In addition, zinc particles can enhance micro/nanomotor propulsion through the galvanic effect with metal particles. In one study, a Janus gallium/zinc (Ga/Zn) micro/nanomotor exhibiting excellent biodegradability and biocompatibility was developed [59] by asymmetrically coating liquid metallic Ga on Zn particle surfaces. In an acidic solution simulating gastric acid, the hydrogen, which reacted with the zinc and acid, enabled the micro/nanomotor to self-propel up to 383 μm/s by generating air bubbles.

2.1.4 Au

When stimulated by endogenous substances, Au cannot generate bubbles because its catalytic activity is not as powerful as that of Mg and Zn. However, Au does exhibit good heat conversion ability and can be employed as a micro/nanomotor driving mechanism.

By exploiting the good photothermal properties of Au, an NIR photodynamic Janus mesoporous silica nanomotor (JMSNM) micro/nanomotor comprising

an MΦ cellular membrane was developed [60]. Owing to the asymmetry of the Au half-shell, a photothermal effect was generated when the JMSNM micro/nanomotor was exposed to NIR light, and the thermal gradient generated by the photothermal effect crossed the Janus boundary of the JMSNMs and generated a self-heating kinetic force that pushed the JMSNMs. Through the same mechanism, the asymmetrical distribution of Au could generate photothermal conversion by irradiation with an external light source. Shao *et al.* designed erythrocyte-membrane-encapsulated Janus polymer motors, which self-propelled when exogenously stimulated by NIR light [61]. These micro/nanomotors comprised heparin (Hep) and CHI, and the surface was modified by an erythrocyte membrane. The capsule was formed by opposite charges on the surface, and both natural polymers were assembled layer by layer (LbL). To propel the micro/nanomotor under fuel-free conditions, LbL capsules were partially wrapped in gold shells. When the capsules were irradiated using NIR light, a partial thermal gradient was generated owing to the asymmetrical Au modification, which produced a thermophoretic effect that drove the micro/nanomotor motion. Recently, researchers have fabricated NIR-driven JMSNMs [62] by doping MSNPs with gadolinium and depositing Au on the hemispherical NP surface. Again, owing to the asymmetry of the Au half-shell, an asymmetric thermal gradient was generated by irradiation with NIR, and the nanomotor achieved efficient self-propulsion. Using the same photothermal conversion propulsion mechanism, Lin *et al.* designed an NIR light-propulsion Janus-based nanoplatform (**Figure 2B**) [63]. Au half-shell-covered Janus nanomotors were loaded with an endophagy adjuvant (MnO₂ nanosheets) to produce microRNAs (miRNA)-responsive hairpin DNA quadrilateral-nanostructured probes through catalytic hairpin assembly. Surface plasmon resonance absorption generated a thermal gradient on the Au half-shell of the nanoplatform, which promoted thermophoresis.

2.1.5 Metallic compounds

In addition to frequently employed Pt metal particles, some common metallic compounds, such as MnO₂, can catalytically decompose hydrogen peroxide to generate gas and, therefore, propulsion. Additionally, Fe₃O₄'s characteristics enable magnetically controlled propulsion. Owing to its strong photocatalytic characteristics, bismuth oxyiodide is also a key material for application to micro/nanomotors.

In one study, a micro/nanomotor exhibiting double-layered microtubes was designed using

electrochemically reduced graphene oxide/MnO₂ [10]. Owing to the rough inner surface and porous structure of the microtubes, the micro/nanomotor exhibited good catalytic activity, which could decompose H₂O₂ to generate gas and achieve rapid and efficient propulsion. Chen *et al.* used naturally abundant kapok fibers (KFs) as a template to design a manganese dioxide (MnO₂)-catalyzed tubular micro/nanomotor (**Figure 2C**) [64] wherein MnO₂ was deposited and modified on the inner and outer walls of the KFs. Hydrogen peroxide (H₂O₂) was catalytically decomposed using MnO₂, and oxygen (O₂) bubbles were generated to self-propel the micro/nanomotor. Similarly, Yang *et al.* developed a magnetic micro/nanomotor using natural KFs as a template to uniformly grow laccase-immobilized Fe-BTC (Iron 1,3,5-benzenetricarboxylate) metal organic framework (MOF) NPs on Mn₂O₃-NiFe₂O₄ nano-sheets [65]. The micro/nanomotor used the catalytic effect of Mn₂O₃ on H₂O₂ and moved at 120 μm/s under the action of decomposing gas. By exploiting the excellent photocatalytic properties of bismuth oxyiodide (BiOI), a BiOI-based JM was fabricated [16]. The micro/nanomotor could be activated by irradiation with visible light, including blue and green wavelengths in broad-spectrum light, and was developed using only biotechnology. Therefore, the micro/nanomotor could undergo a photocatalytic reaction in pure water without adding any chemical fuels. The micro/nanomotor was propelled, and the photocatalytic driving force was regulated by changing the visible-light power. Additionally, magnetic fields have been used to propel micro/nanomotors. Xie *et al.* developed a strategy for programming hematite colloidal particles into microrobot swarms in liquids, chains, vortices, and ribbons in alternating magnetic fields [66]. Peanut-like hematite colloidal particles exhibiting long and short axes of 3 and 2 μm, respectively, could form numerous microrobots. The short axis of the microrobots exhibited permanent momentum. In the absence of external stimuli, the microrobots naturally aggregated into a mass owing to their intrinsic magnetic dipole forces. An external rotating magnetic field could produce circular polarization on any plane in three-dimensional (3D) space, thereby exciting the microrobots to achieve different motions (such as oscillation, swinging, rolling, spinning, and tumbling). In one study, calcium-crosslinked degradable alginate (Ca-Alg) hydrogel capsules were prepared utilizing a hydrodynamically electrospraying ionization jet assisted by low-frequency ultrasound [67]. The ultrasound increased the capsule uniformity, and the formation of a gel layer was simultaneously prevented at the air-water interface. The capsules

were used to encapsulate model drugs, and monolayer polylactic acid was applied as a sealant. The capsule propulsion was guided by adding superparamagnetic magnetite particles (Fe₃O₄) to the capsule and applying a stable or an alternating oscillating magnetic field. By applying an exogenously stimulating magnetic field, Wang *et al.* recently used an easily fabricated and versatile setup to design magnetic helical hydrogel micro/nanomotors (PVA@Fe₃O₄@CXCL12) [68]. Magnetic ferric oxide NPs were embedded in the hydrogel micro/nanomotor, which enabled the remote operation and actuation of the micro/nanomotor through the magnetic field. The wireless control conveyed biocompatibility to the hydrogel motor. In addition, Li *et al.* designed semiartificial magnetotactic bacteria (SAMTB), which exhibited a tunable magnetic moment and good sensitivity [69]. Synthesized Fe₃O₄ magnetic NPs (MNPs) were attached to the surfaces of *Magnetospirillum magneticum* AMB-1 (AMB) and magnetotactic bacteria (MTB) at a high usage rate. Fe₃O₄ MNPs were mainly connected to AMB-1 through electrostatic interactions. By varying the concentration, size, and surface charge of MNPs, the bulk magnetism of the SAMTB could be manipulated to control magnetic sensitivity and mobility. Wu *et al.* designed a chemical/magnetic hybrid micro/nanomotor based on Fe₃O₄ MNPs and GOx-modified cubic calcium carbonate microparticles (CCMPs) [70]. The GOx enzymatic reaction functioned as a motor device using both starvation therapy and glucose as fuel, which enabled the hybrid micro/nanomotor to self-propel. Additionally, owing to the incorporation of Fe₃O₄ NPs, which played the role of a magnetic motor, the kinetic energy of the micro/nanomotor increased. The device exhibited both chemical and magnetic engines, which drove the motion. Owing to graphene oxide (GO) photocatalytic properties, a cuprous oxide@GO (Cu₂O@GO) micro/nanomotor was introduced for high-efficiency actuation under different light conditions [71] using various biocompatible fuels (e.g., glucose, leucine, and urine). The addition of GO to the micro/nanomotor enhanced the photocatalytic performance, which enabled efficient propulsion under visible, and even NIR, light.

2.1.6 Multiple metals

In addition to hydrogen peroxide and water, glucose is a relatively common endogenous stimulant in the living body. After decomposition, oxygen is generated to propel micro/nanomotors. Owing to their unique catalytic properties, Au and Pt bind at specific positions in the same nanostructure to achieve synergistic catalysis by colocalizing different active

sites. Kwon *et al.* introduced an Au/Pt-based Janus nanostructure resembling an “egg-in-nest” morphology (Au/Pt-Ens) [72]. The nested Pt structure was asymmetrical: The bottom was closed and nested by Au NPs, and Au NPs fixed the nested Pt structure in place. The nested morphology and large openings in this nanostructure increased the entry of the fuel (glucose) and mass transfer of the product, and the nanostructure [Au-Pt] active site was at one end of the NP. The concentration gradients at the cavity and outer surface competed to govern the nanostructure mobility. Researchers have previously prepared uricase-powered Janus upconversion NP-SiO₂ micro-motors (JUS motors) by asymmetrically immobilizing enzymes and upconversion NPs on silicon microparticle surfaces [73]. Owing to the asymmetrical distribution and bilateral structure of the enzymes, the JUS motors could autonomously move, driven by the uric acid in urine. Because some micro/nanomotor constituent materials are magnetic, propulsion was achieved by applying magnetic fields [74]. Iron (Fe) and platinum (Pt) were codeposited to prepare ferromagnetic FePt nanopropellers. The main nanopropeller components were FePt and silica, and the nanopropellers were driven by gradient-free rotating millitesla fields. Owing to their high magnetic moment, the FePt nanopropellers exhibited a propulsion velocity superior to those of both the Fe- and Ni-based magnetic propellers. Light is among the most used exogenous stimuli. Some researchers have found that under the combined action of light irradiation and an electric field, the micro/nanomotor velocity can be greatly improved. Researchers previously designed a TiO₂ - Pt Janus microspheres (Figure 2D) to drive a photocatalytic titania - platinum (TiO₂ - Pt) micro/nanomotor under the combined action of light and an alternating current electric field [75]. Invariably, the systemic velocity was more rapid than the sum of the individual velocities under any other propulsion.

Although the development of micro/nanomotors has excellent application prospects, several obstacles must still be overcome. The propulsion or application of micro/nanomotors is difficult because the key materials required for fabricating micro/nanomotors are restricted or constrained by the endogenous or external stimulation these materials require. For instance, owing to its excellent photo-thermal conversion ability, Pt, which is frequently employed in such systems, also has drawbacks. Pt catalysts are expensive, hazardous, unstable, and scarce, which severely limit the application potential of Pt catalysts [76]. Similarly, Au NPs are costly. Although Mg exhibits numerous positive inherent properties, numerous important obstacles must be

overcome before it can be employed in challenging practical applications. Notably, the rapid consumption of magnesium during actuation and small micro/nanomotors usually result in a short lifespan for Mg-based motors. Numerous measures can be used to extend the lifespan of Mg engines, including reducing the bubble formation frequency by rationally allocating micro/nanomotor compositional characteristics (e.g., upgrading the opening shape and size) or alloying with other metals and reducing the corrosion rate by reducing the number of pitting-induced anions. Additionally, the consideration of how Mg micro/nanomotors release hydrogen bubbles is important. The assessment of this latent negative effect is crucial for *in vivo* applications because the danger from the formation of gas embolisms in blood arteries is considerable owing to the relatively poor solubility of H₂ in water. Undeniably, excess Mg ions can cause hypermagnesemia, which exhibits symptoms such as nausea, muscle weakness, a low heart rate, and hypotension. Additionally, excess Mg ions can increase the local osmotic pressure, which can disturb cellular homeostasis. Before magnesium micro/nanomotors can be therapeutically applied, these problems must be solved [77]. Zn NPs have been used as essential components for manufacturing nanomotors. Zn exhibits high metallic catalytic activity, which enables it to react with gastric juice protons to produce gas and release numerous hydrogen bubbles. However, because Zn-based systems readily corrode, their lifespans are shortened [56]. The primary components that power nanomotors fundamentally comprise elementary metallic NPs, which makes such nanomotors both expensive to produce and potentially harmful to living organisms and biological cells. However, these drawbacks can be avoided using porous and mesoporous materials loaded with compound NPs, such as Fe₃O₄ or MnO₂. Fe₃O₄ exhibits magnetic properties that enable good control accuracy when utilizing magnetic fields, which can be used to construct nanomotors for accurately delivering drugs. Subsequently, nanomotors can be recycled by applying magnetic Fe₃O₄ particles, which are also very biocompatible. MnO₂ particles decompose hydrogen peroxide (H₂O₂) fuel to produce oxygen bubbles and generate the necessary mechanical force for operating motors. MnO₂ motors are favored for their low cost, simple production, wide range of fuel concentrations, adjustable geometry and size, long lifetime, high efficiency, and programmable crystal structure and surface topography. For water filtration, MnO₂-based micro/nanomotors play dual roles of catalytic decomposition and adsorption-bubble separation. However, few studies have examined MnO₂ as a catalyst. Many

hybrid micro/nanomotors employ two key materials. Recent developments in hybrid micro/nanomotors have attracted considerable research attention. Considering various energy sources that micro/nanomotors can utilize, hybrid micro/nanomotors activated by multiple power sources can switch between two or more driving forces, which enables motors to accelerate/decelerate, move forward/backward, and/or switch motion modes [75]. Composite NPs are prepared by depositing two or more metals, a combination of metal and compound, or two or more compound NPs on special nano/microspheres through a certain method. Alternatively, this means two or more substances are used as key materials for driving micro/nanomotors. Although the cell absorption capacity and movement velocity of composite NPs are higher than those of single-metal NPs [78], such systems exhibit the same problems as those of simple metal NPs. That is, owing to the scarcity of precious metal resources, certain metals are more expensive and can be toxic to living organisms or biological cells. Magnesium-based micro/nanomotors driven by a dual mechanism are propelled by the reaction between Mg and H₂O. Pt decomposes when it encounters H₂O₂, which prolongs the motion life. Owing to the asymmetric Pt coating, the corrosion of the active metal (Mg) is decelerated, and the micro/nanomotor life is prolonged. In addition, the micro/nanomotor exhibits high toxicity and precious metal scarcity [79]. Furthermore, compared with Au and Ag NPs, Fe ones are feasible for driving micro/nanomotors. Moreover, micro/nanomotor driving requires the use of H₂O₂ as a fuel source, which is toxic to living cells. However, instead of using H₂O₂, Au/Pt-Ens can oxidize glucose and generate O₂ gas, which reduces the toxicity to living cells and organisms [72]. Additionally, Au/Pt-Ens can overcome stochastic Brownian forces while imparting lifelike directed mechanical motion; is biologically nontoxic; and uses plentiful fuels, such as glucose. However, the fabrication of such micro/nanomotors is costly and requires the research and development of inexpensive metals to achieve the same effect. Ferromagnetic FePt nanomotors, which are noncytotoxic and biocompatible, exhibit a remanence and magnetization comparable with those of permanent NdFeB micromagnets [74]. Magnetic particle systems are particularly promising because they can be manipulated by magnetic fields. The face-centered tetragonal (fct) L1₀ phase of FePt is a promising magnetic material, which is noncytotoxic, nonimmunogenic, and highly biocompatible and exhibits a strong magnetic residue. FePt is a chemically stable rare-earth-free permanent magnetic material exhibiting high magnetic crystal anisotropy.

FePt NPs exhibit high remanent magnetization, saturation, energy production, and coercivity. Chemical/magnetic hybrid micro/nanomotors can be fabricated using Fe₃O₄ MNPs and GOx-decorated CCMPs [70]. Fe₃O₄ NPs were incorporated into a hybrid micro/nanomotor intended to function as a magnetic motor and not only enhanced the kinetic energy of the device but also controlled the motion direction. The motor was propelled by glucose, a typical bioavailable and biocompatible fuel, and was activated by a magnetic field. The magnetic and chemical engines both improved motor behavior, provided propulsion, and enhanced cellular uptake. Simultaneously, the GOx-initiated biocatalytic reaction consumed intracellular glucose, which further reduced cancer cell viability. Additionally, Fe₃O₄ is economically feasible. Cu₂O@GO micro/nanomotors featured localized light-induced thermal effects and enhanced photocatalytic performance; that is, this motor could be operated under NIR irradiation with a broad range of biocompatible fuels, such as leucine, glucose, and urea solutions [71]. For this photocatalytic micro/nanomotor, the excitation wavelength extended to NIR light. This strategy for improving the performance of light-driven micro/nanomotors by GO doping opens an avenue for fabricating micro/nanomotors showing excellent potential for bioenvironmental applications.

2.2 Nonmetallic nanocomplexes

2.2.1 Inorganic nonmetallic compounds

In contrast to metallic nanocomposites, inorganic nonmetallic compounds frequently appear in micro/nanomotors that rely on the photothermal conversion of essential components under exogenous light stimulation. For instance, GO and g-C₃N₄ are photocatalytic materials that enable photothermal conversion to power micro/nanomotors in electromagnetic fields.

Oil-in-water emulsion templating, adopted by Wang *et al.*, was sufficiently simple and versatile to fabricate an emulsion-hydrogel motor comprising a hydrogel matrix and low-boiling-point fuel-oil emulsion [80]. Under stimulation, the thermally induced phase transition can generate bubbles that are violently ejected from one side of the motor to achieve efficient propulsion. Such motors can be integrated with Fe₃O₄ NPs for magnetic guidance. Under NIR light conditions, the addition of GO (**Figure 3A**) can control the distance and accurately regulate the motion of motors, including the orientation, velocity, and trajectory. Additionally, reduced-GO aerogel microspheres can function as power devices [81]. In that study, microspheres were produced using electrospray ionization, which is

simple to operate, and the systems exhibited size controllability and an isotropic structure. In water, graphene can convert light to heat in an externally stimulated asymmetric light field and drive a micro/nanomotor because of the asymmetric thermal gradient generated in water. Furthermore, $g\text{-C}_3\text{N}_4$ is a promising photocatalytic material characterized by a metal-free structure, good thermochemical stability, and visible-light responsiveness [82]. Dong *et al.* combined $g\text{-C}_3\text{N}_4$ photocatalysts and self-propelled jet carbon micro/nanomotor carbon bottles utilizing infrared light and active mass transfer to enhance the

photocatalytic performance of the micro/nanomotor [83]. When stimulated by light, the combination exhibited improved motility and excellent self-propulsion.

2.2.2 Organic compounds

Numerous chemical molecules require exogenous stimulation for propelling motors. Although some chemicals are micro/nanomotor components, they may also be employed as raw materials for driving those micro/nanomotors, and micro/nanomotors can be promoted by producing gas.

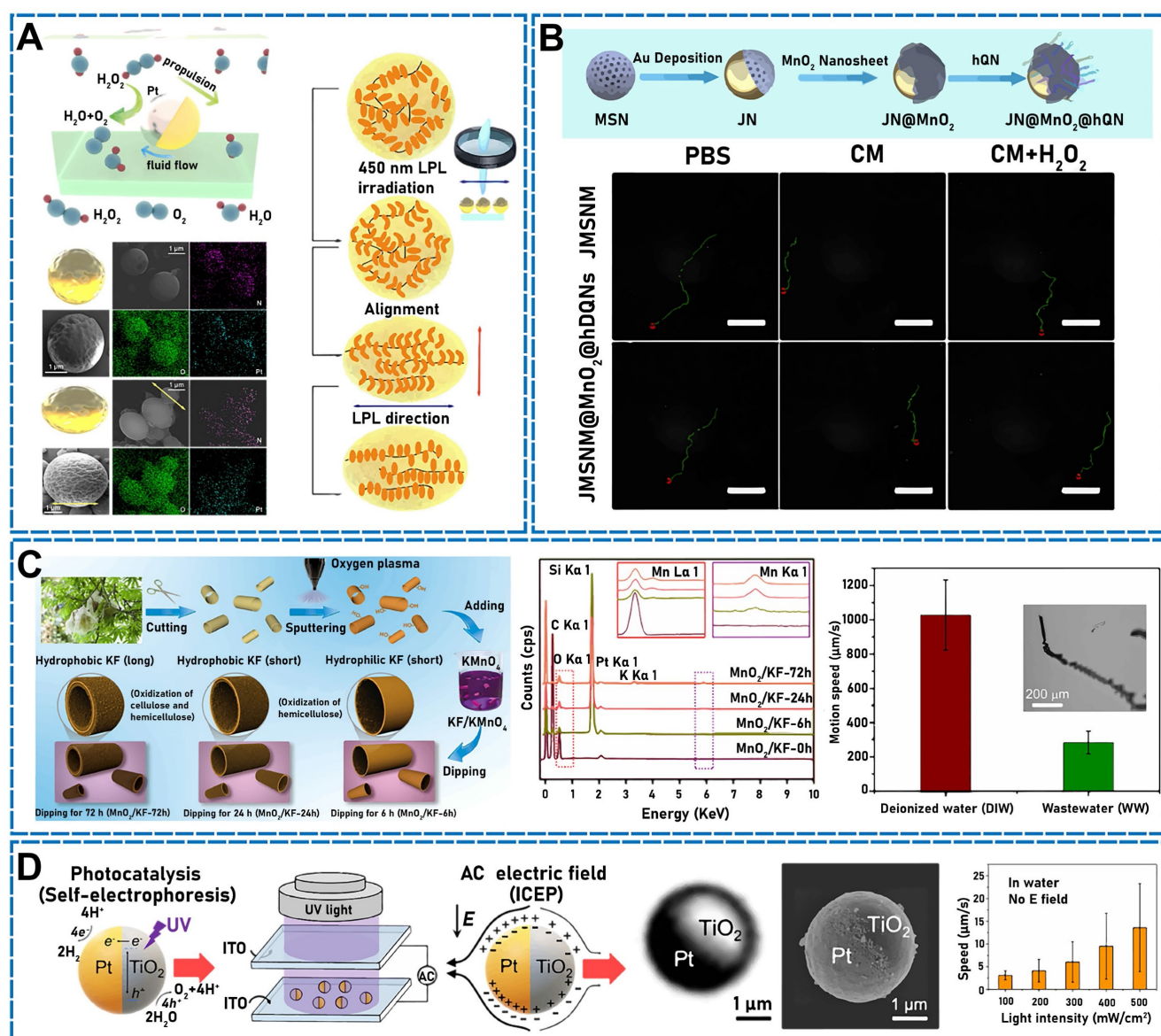


Figure 2. (A) Self-propulsion mechanism of Pt-PAzoMA. Scheme and SEM images of micro/nanomotors with EDS mapping. The deformation mechanism of the micro/nanomotors. Reproduced with permission [47]. Copyright 2021, American Chemical Society. (B) Design of $\text{JN@MnO}_2\text{@hQN}$ nanoplatform and imaging of miRNAs in Cells. Trajectory states of JN and $\text{JN@MnO}_2\text{@hQN}$. Reproduced with permission [63]. Copyright 2021, American Chemical Society. (C) Fabrication of our MnO_2/KF micro/nanomotors. EDX spectra of the MnO_2/KF micro/nanomotors. Motion speeds of micro/nanomotors. Reproduced with permission [64]. Copyright 2021, American Chemical Society. (D) Working mechanism of the $\text{TiO}_2\text{-Pt}$ hybrid micro/nanomotor. Optical micrograph and SEM of a $\text{TiO}_2\text{-Pt}$ Janus microsphere. Speeds of a $\text{TiO}_2\text{-Pt}$ micro/nanomotor in light. Reproduced with permission [75]. Copyright 2020, American Chemical Society.

Inspired by the well-established model of dye-sensitized solar cells, light-driven artificial microfilaments can be produced and derive energy from visible light, which enables propulsion and navigation under visible-light conditions. Zheng *et al.* designed and developed a motor that absorbed visible-light photons when a photosensitizer (organic dye) was loaded into titanium dioxide, and electrons were injected from it into titanium dioxide nanowires, which generated a propulsive photocurrent [84]. In addition to their photothermal conversion properties, some organic compounds can be used as raw materials to drive micro/nanomotors while simultaneously being used as micro/nanomotor components. An NO-gas-driven nanomotor originally comprising hyperbranched polyamide/L-arginine has previously been developed [85]. The micro/nanomotors comprised endogenous biochemical reactions in living organisms, which converted the amino acid L-arginine to nitric oxide (NO) in the presence of NO synthase (NOS) or reactive oxygen species (ROS). Some organic compounds can be stimulated using sound fields. Ye *et al.* found that a Janus mesoporous SiO₂ nanorod partially coated with gold (Au NR-mSiO₂) deeply penetrated tumor tissue under exogenous stimulation with ultrasound [86]. When 2,2-azobis[2-(2-imidazolin-2-yl) propane] dihydrochloride (AIPH) was ultrasonicated in mSiO₂ (Au NR-mSiO₂/AIPH), a high-efficiency N₂ microbubble developed and drove the nanomotor. Air bubbles (such as O₂, H₂, and NO) can be used as the propulsion power source and play an indispensable role in physiological activities [87]. Deng *et al.* designed a hollow asymmetric polydopamine (PDA) NP and modified it with the Cys-Arg-Glu-Lys-Ala (CREKA) peptide, namely, BNN6@PDA@CREKA (B@P@C), to form a donor for loading NO (**Figure 3B**) [88]. The resulting micro/nanomotors efficiently aggregated at thrombus sites [89]. The micro/nanomotor absorbed NIR light, and the release of NO bubbles rapidly moved the micro/nanomotor and enabled the deep penetration of thrombi by transferring energy to the NO donor (BNN6 (*N,N'*-di-sec-butyl-*N,N'*-dinitroso-1,4-phenylenediamine)) to achieve a thrombolytic effect. C₃N₄ is a common inorganic polymer photocatalyst, which can photocatalytically hydrolyze water. In one study, a visible light-driven micro/nanomotor comprising binary photocatalytic carbon nitride (C₃N₄) and photothermal polypyrrole NPs (PPyNPs) was developed under fuel-free conditions [90]. Owing to the excellent photocatalytic properties of C₃N₄ and photothermal effect of PPyNPs, this micro/nanomotor was driven by two independent but competing mechanisms, namely, self-diffusion and autothermal

electrophoreses.

To advance micro/nanomotors, photothermal conversion must typically be induced under the influence of external light. Without the use of any additional chemicals, light is transformed into mechanical energy throughout the process [16]. Although infrared light can comprise over 50% of solar radiation, it cannot directly initiate photocatalytic activity owing to its low photon energy [91]. Because heat can be used to power micro/nanomotors, infrared light exhibits a high photothermal conversion efficiency (over 85%) [92]. Reduced GO (RGO) is a typical graphene-based material that exhibits extraordinary qualities, such as high thermal conductivity, a large surface area, and electrical conductivity. These attributes make RGO a comparatively excellent candidate for high-tech micro/nanomotor applications. Additionally, RGO can efficiently collect NIR photons and quickly convert them to heat energy through the photothermal effect. Previous studies have shown that owing to their porous, multilayered, and hydrophobic structures, RGO-based aerogel microspheres exhibit an exceptional adsorption capacity and ultralow density and might, therefore, be used for treating environmental pollution or delivering medicines. When externally stimulated by asymmetric NIR light, graphene may use photothermal conversion to generate an NIR-induced self-asymmetric thermal gradient in water, which can then be used to power a micro/nanomotor. Owing to its high thermochemical stability, metal-free structure, and visible-light responsiveness, g-C₃N₄ is a typical photocatalytic material that shows tremendous application potential. However, g-C₃N₄ exhibits a modest hydrogen production efficiency, and its photocatalytic performance must be enhanced using numerous methods. The human body naturally contains organic substances, such as L-arginine and PDA. The metabolic process through which NOS and other ROS convert L-arginine to NO in the human body has garnered interest. L-arginine exhibits immunomodulatory properties that stop the thymus from deteriorating and encourage the development of thymic lymphocytes. However, because hydrogen peroxide is hazardous, an alternative fuel must be found in live cells or organisms. L-arginine can be used as a fuel for tiny, NO-powered micro/nanomotors. The produced NO is used for propulsion and exhibits beneficial effects, such as encouraging endothelialization and anticancer actions. As a fuel, L-arginine does not generate any waste and shows potential for biological applications, such as the treatment of a range of conditions in various tissues, including cancers and blood vessels [85]. Similar to L-arginine, PDA transfers energy by absorbing NIR

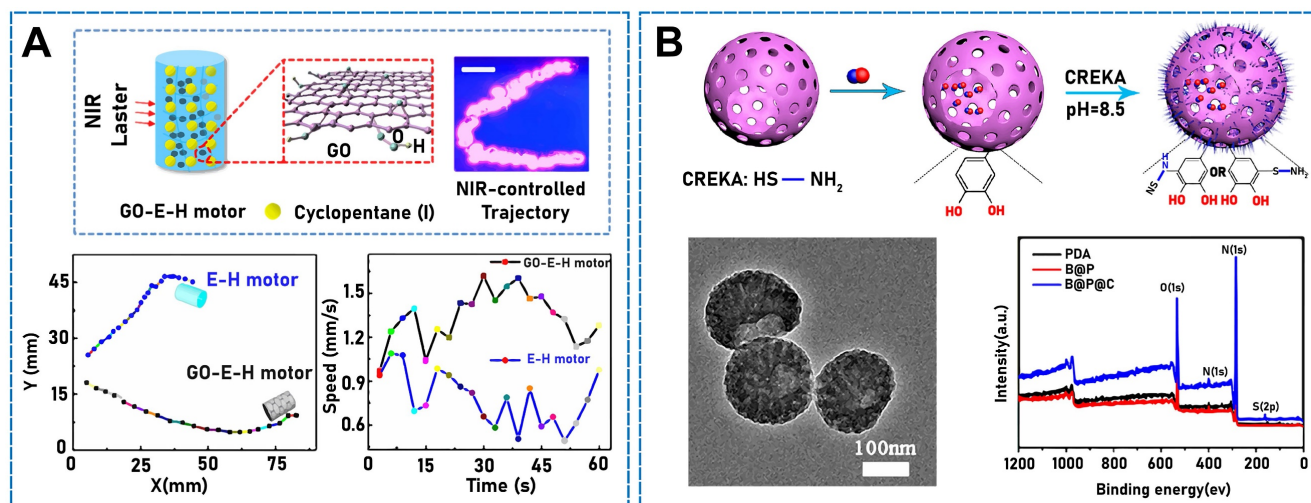


Figure 3. (A) The composition of GO-E-H-motor. The trajectories of a GO-E-H-motor. The velocity of a GO-E-H-motor. Reproduced with permission [80]. Copyright 2017, American Chemical Society. (B) Preparation process of B@P@C nanosweeper. TEM images of B@P@C nanosweepers. XPS of PDA, B@P, and B@P@C. Reproduced with permission [88]. Copyright 2021, American Chemical Society.

light, which releases NO bubbles. However, owing to its high light-conversion efficiency, the micro/nano-motor functions as a photothermal agent to accelerate the dissolution of blood clots, which results in a combination of mechanical and photothermal thrombolysis [89].

2.3 Enzymes

The application of nanozymes (which have capabilities resembling those of enzymes, such as catalase, oxidase, peroxidase, and superoxide dismutase) greatly broadens the scope of micro-electromechanical chemical fuels [93]. Because they can control velocity with remarkable accuracy, enzyme-based nanomotors are extremely important [94]. Nanozyme-driven micro/nanomotors offer a wide range of intriguing applications [95]. Enzymes enable conversion between chemical and mechanical energies and are found in numerous organisms. The application of enzymes as biocatalysts to power micro/nanomotors is an important concept. Compared with conventional reaction fuels, fuels used by enzyme-driven micro/nanomotors exhibit superior bioaffinity, good biocompatibility, and considerable potential for biomedical applications. When enzymes are loaded on artificial tubular micro/nanoparticles or spherical particle structures, synthetic enzyme-powered micro/nanomotors (EMNMs) can be catalyzed by enzymes to achieve diverse functions in complex environments [96].

2.3.1 Urease

In enhanced enzyme diffusion and chemotaxis, many enzymes spread more quickly in the presence than in the absence of substrate fuels. Therefore, enzymes can be employed as active molecules [97].

Because blood contains urea, urease is a crucial component of molecular motors.

Using silica spheres, Hortelão *et al.* prepared core-shell MSNPs, 3-aminopropyltriethoxysilane-functionalized MSNPs, and MSNP-NH₂ NPs. The surface exhibited free amino groups, and glutaraldehyde was used as a linking molecule for covalently attaching urease to the NPs and producing urease micro/nanomotors. The urease on the micro/nano-motor surface decomposed urea to ammonia and carbon dioxide, which self-propelled the motors [98]. In addition, in a previous study, fiber rods were fabricated using a unique Janus structure and double-sided electrospinning wherein urease and folic acid were conjugated to both sides of Janus rods (JRs) as power sources [99]. The urease implantation density determined the movement velocity and trajectory of the JMs, and large mean-squared displacements and high movement velocities were detected in both the extracellular matrix, mimicking tumor tissue, and phosphate-buffered saline. With increasing urease density, the propulsion force also increased. Using endogenous urea stimulation, Tang *et al.* designed a Janus platelet micro/nanomotor, which asymmetrically immobilized urease on the surface of native platelet cells [100]. Owing to the asymmetrical distribution of the urease on platelet cells, the urea did not disintegrate uniformly in the biological fluid, which enhanced the chemical electrophoretic motion. Similarly, urease-micro/nanomotor-driven Janus-Nes systems have recently been synthesized by asymmetrically immobilizing urease on the surface of natural Nes followed by loading urokinase (UK) (Figure 4A) coupled with Ag NPs (Ag-UK) [1]. The urease-catalyzed endogenous urea produced ammonia and carbon dioxide, which

propelled the system. In addition to the attachment of urease to NPs, Jiao *et al.* recently developed asymmetrically modified urease in yeast cells [101]. With urea as an endogenous stimulus, self-propulsion was achieved owing to the asymmetrical modification of yeast cells.

2.3.2 Catalase

Because hydrogen peroxide is toxic to cells and tissues, the application of catalase to drive nanomotors and achieve self-propulsion has become a very important research topic. For example, in one study, a high-efficiency enzyme-powered micro/nanomotor was designed and fabricated by combining catalase with a PEDOT⁺ and sodium 4-styrenesulfonate)/Au microtube (PEDOT-PSS/Au) [102]. The inner surface of the tube (PEDOT-PSS/Au) was assembled in multiple layers. The micro/nanomotor exhibited efficient movement through stimulation with hydrogen peroxide. Using the same propulsion principle, Wang *et al.* fabricated drug-loaded PLGA micro/nanomotors asymmetrically covered with enzymes (in a patch-like distribution) applied by electrospraying and prepared using 1-ethyl-3-(3-dimethylaminopropyl)carbodiimide coupling and then postfunctionalized with catalase [103]. A H₂O₂ gradient can sustain the directional movement of nanocarriers, including enzymes, toward high-concentration fuels. With increasing fuel amount, the micro/nanomotor velocity also increases. In addition, micro/nanomotors can be asymmetrically grafted by catalase. In a previous study, JMs were prepared by grafting catalase on the side of JRs to power JMs by catalyzing H₂O₂ decomposition [104]. Catalase (CAT) was covalently bound and immobilized on one side of JRs, and a TLS11a aptamer was covalently bound to JMs. The catalytic reaction of CAT with hydrogen peroxide can propel JMs. In another study, researchers grafted CAT on one side of Janus fiber rods (JFRs) and combined mannose on the other side [105]. The CAT decomposed the hydrogen peroxide to generate oxygen bubbles and propel JMs. In contrast to grafting, CAT can also encapsulate JFRs to generate oxygen by decomposing hydrogen peroxide and propel a micro/nanomotor. An ultrasmall-cell ($\varnothing \sim 150$ nm) nanomotor has previously been developed and encapsulated in CAT for application to biocatalysts [106]. The device decomposed H₂O₂, and the generated O₂ was used as a power supply. Likewise, Yang *et al.* designed an enzyme-powered porous micro/nanomotor constructed from MOFs, as shown in **Figure 4B** [107]. First, presynthesized microporous UiO-type MOFs were ozonated, and CAT was then used to encapsulate mesopores. In H₂O₂, MOF engines undergo an

enzymatic reaction, which produces oxygen bubbles to propel the motor.

2.3.3 Multienzymes

Because urease, CAT, and glucose oxidase (GOx) are the three most often used biological enzymes, multienzyme-driven nanomotors can be used to synthesize various biocompatible enzymes into a micro/nanomotor that functions as a biocatalyst to produce propulsion when substrate fuels are present.

Because the use of enzymes to propel micro/nanomotors requires fuel (water, hydrogen peroxide, urine, glucose, *etc.*), multienzyme-driven micro/nanomotors are necessarily fuel-dependent. Previously, a hybrid micro/nanomotor has been synthesized using CAT and urease [108]. Biotin-streptavidin ligation was used to functionalize polystyrene microparticles with both urease and CAT. Particle diffusion increased with increasing matrix concentration, and the diffusion of CAT- and urease-coated particles also increased with increasing substrate concentration. Not only can urease and CAT be mixed, but CAT and GOx are also another common combination. Gao *et al.* designed a carbonaceous nanoflask (CNF) motor (**Figure 4C**) that moves spontaneously in glucose. The motor power was provided by the cascade reaction between GOx and CAT [109]. By controlling the nanomotor's surface wettability, the micro/nanomotor can move in a certain direction. To enable propulsion, a hydrophobic CNF motor was developed to move from the round bottom to the opening neck (backward), and a hydrophilic version was developed to move from the opening neck to the round bottom (forward). In a different study, scientists developed a core-shell nanomotor exhibiting dual-enzyme functionality (designated as UTZCG) [110]. The nanomotor featured a metalorganic NP framework that enhanced the complementary effects of starvation and photodynamic therapies. In the catalytic cell, glucose was decomposed by modified GOx to starve cells, and H₂O₂ was produced. Subsequently, CAT catalyzed H₂O₂ decomposition, leading to propulsion.

In nanozymology or nanomaterial catalysis [111], enzyme-catalyzed reactions play a facilitating role [112]. In living organisms, enzymes convert chemical to mechanical energy and facilitate other biochemical reactions. The application of enzymatic biocatalysts to power micro/nanomotors is a novel approach. Enzymatic reaction fuels are more ecofriendly and degradable than traditional fuels, and enzyme-powered micro/nanomotors show potential for biomedical application breakthroughs owing to their biocompatibility. However, enzymes have several drawbacks; for instance, although CAT-driven

EMNMs can move rapidly owing to bubble propulsion, hydrogen peroxide is toxic to living cells. Various EMNMs can be driven by urease, CAT, and several other enzymes because key EMNM materials can perform on-demand tasks. The more common biological enzymes are urease, CAT, and GOx, which are found widely in nature, not only in animals but also in plants. Although many enzymes exhibit the same inherent properties that could enable the enzymes to be used as motors for autonomous movement, most enzymes exhibit limitations that hinder the control of their motor behavior, which limits their practical application. Clearly, natural EMNMs are not designed to accomplish the intricate operations or specific tasks required for guided locomotion. To be useful, enzyme-driven micro/nanomotors must improve their propulsion and overcome various limitations in complex environments. Currently, the methods most used to improve the driving force are the improvement of the enzyme catalytic ability by modifying the motor shape to accommodate hydrodynamics (e.g., improving the enzyme catalytic unit) and the utilization of cascade reactions with two or more enzymes. A combination

of more advanced and intelligent testing or analytical techniques will be required to elucidate the energy conversion mechanisms of enzymatic reactions and generate the driving force. This would provide a theoretical basis and strategic guidance for subsequently studying EMNMs exhibiting more advantageous propulsion capabilities [96].

2.4 Living cells

The design, propulsion, and application prospects of cellular micro/nanomotors have considerably advanced [113]. To develop synthetic micro/nanomotor applications that can function in biological systems without causing harm, biocompatible and biomimetic micro/nanomotor devices are required [114]. Researchers have developed different artificial micro/nanomotor cells that imitate micro/nanomotors. Synthetic micro/nanomotors can be functionalized with various cellular elements, such as membranes, to assume cellular traits [115-117]. Flagella, such as those on sperm, synthetic bacteria and MTB, inventive magnetic filaments, and bacteria-driven microrobots, are used for low-Reynolds-number propulsion [118].

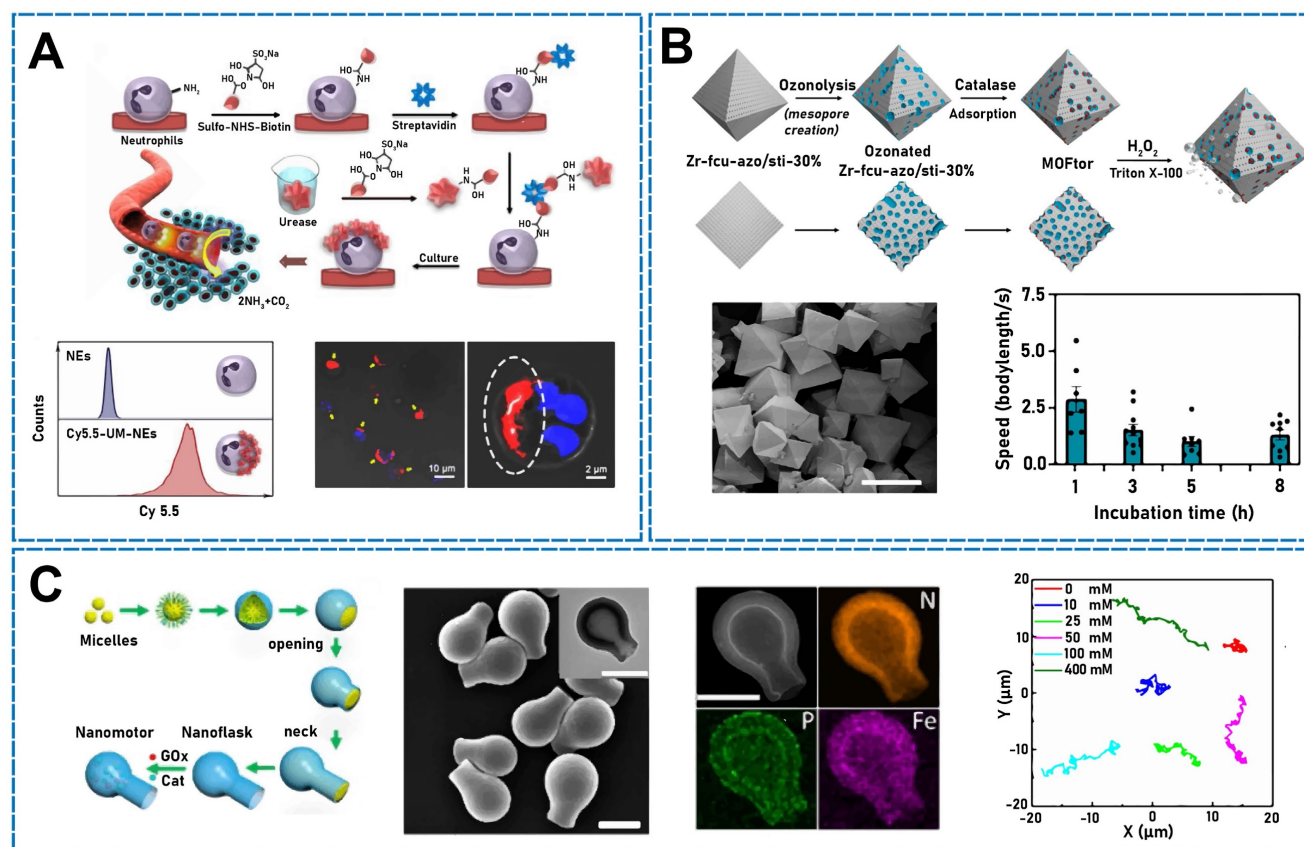


Figure 4. (A) The preparation principle of urease motor. Fluorescence imaging of UM-Cy5.5-Nes. Flow cytometry histograms of UM-Cy5.5-Nes and controlled Nes. Reproduced with permission [1]. Copyright 2022, American Chemical Society. (B) Schematic diagram of the synthesis process of MOFtors. FESEM image. Speed of MOFtors at different incubation times. Reproduced with permission [107]. Copyright 2020, American Chemical Society. (C) Synthesis of enzyme-loaded round-bottom CNF motors. SEM image of L-CNFs. STEM and EDX mapping images of the enzyme-loaded hydrophilic CNF motors. Trajectories of the hydrophilic CNF motors at different glucose concentrations. Reproduced with permission [109]. Copyright 2019, American Chemical Society.

2.4.1 Sperm

In the 1950s, Machin emphasized that sperm motility was not accounted for or explained by forcing in the cell membrane but by motors distributed along the flagellum [119]. Magdanz *et al.* combined microtubules and single motile cells to develop a microbiorobot that could be navigated to a prescribed target location [118]. The authors used bovine sperm cells because these cells are similar in size and shape to human ones. The sperm cells entered microtubules and resided in tube cavities. Spermatozoa exhibited very powerful movements and interacted with magnetic microtubules to enable forward movement. Because the bovine sperm cells functioned as the driving force in the hybrid system, autonomous free-swimming functionalized sperm micromotors (FSFSMs) were developed [120]. Natural sperm biomotors have been functionalized using various synthetic nanopayloads, such as endocytosis-particle-modified fluorescein isothiocyanate Pt NPs, CdSe/ZnS quantum dots, and doxorubicin-hydrochloride-coated iron oxide NPs. Under various biological and environmental conditions, FSFSMs exhibited highly effective self-propulsion, and chemoattractant-induced clustering was controlled. The FSFSM velocity was controlled by changing the osmotic pressure of the solution, which changed the flagellum lengths. Similarly, Xu *et al.* used the powerful sperm propulsion as an engine to develop a sperm-mixing micro/nanomotor for precisely delivering drugs [121]. The micro/nanomotor comprised a 3D-printed four-armed magnetic tubular microstructure and a motile sperm cell functioning as a power source and medication carrier, respectively. Furthermore, a quadruped exhibiting four flexible arching arms and a tubular body was developed. Polymer structures were designed using two-photon and 3D nanolithography. Then, a 10 nm iron layer was asymmetrically coated on the tetrapod microstructure inclined at 15° to generate easy axis magnetization. In addition, to improve the composite biocompatibility, a 2 nm layer of titanium was deposited. Previous studies have shown that when the applied arm force was approximately 128 pN, the corresponding displacement was approximately 116 nm, which was sufficient to release sperm [122]. When 450 pN was applied, the displacement rose to 407 nm, which may be produced by hyperactivated spermatozoa (exhibiting an asymmetric beating pattern and larger tail amplitude). Sperm cells function as propulsion sources, while magnetic microstructures are used to guide and release sperm. Additionally, sperm can generate a strong propulsion force and perform rheotaxis/thigmotaxis to swim, which is why

sperm and sperm micro/nanomotors have attracted considerable research interest for bloodstream applications. At the biological microscale, sperm cells are outstanding swimmers. Xu *et al.* developed a hybrid sperm micro/nanomotor (**Figure 5A**), namely, a cap exhibiting a horn-like structure that can not only be assembled with other microcaps for transporting multiple sperm cells but can also be used as an anchoring structure [123]. Streamlined horned caps can maintain the position of sperm micro/nanomotors at rapid blood-flow velocities when sperm are forced toward the channel surface by an external magnetic field. The cap was designed to reduce micro/nanomotor resistance and enable the cap to squeeze past blood cells and through uneven liquids. The motor could actively swim (using continuous pulsatile actions) in the blood flow, and the sperm tiles provided a powerful driving force.

2.4.2 Bacteria

Many bacteria swim in aquatic environments to acquire resources, disperse progeny, and infect hosts. In many bacterial species, motion is driven by a rotating flagellum, which is in turn driven by a bidirectional flagellar motor [124]. At the micrometer scale, bacterial cells can efficiently swim utilizing food sources in their environment. Additionally, bacteria can use synthetic substances for various functions [125]. Researchers have discovered that the *E. coli* envelope can be disrupted and recycled to form nanovesicles. The bacterial envelope protects bacteria from external and dangerous environments [126]. Bacteria are a good example of an elegant and fully self-sufficient natural machine, which swims efficiently, senses the surroundings, finds food, and communicates with other members of the same class. Therefore, to design and perfect functions for application to artificial microdevices, researchers have developed micro/nanomotors that imitate bacteria or directly apply their functions [7].

The attachment of bacteria to the surface of synthesized microparticles is a critical parameter for preparing bacteria-driven microswimmers. To exploit bacteria's excellent and robust autonomous motility and inherent chemotactic behavior as intelligent carriers, scientists have combined bacteria with polymeric beads [127]. Park *et al.* developed a multifunctional, high-performance, bacteria-driven microswimmer (**Figure 5B**) [125]. The main constituents were single *E. coli* cells, which adhered to the surface of drug-loaded, MNP-embedded, multi-layered polyelectrolyte microparticles. The authors found that tuning the viscoelastic characteristics of bacterial surface interactions may be vital for microswimmer movement and bacterial attachment.

In addition, the biohybrid microswimmers exhibited directional motion and skewness under magnetic guidance and chemoattractant gradients, respectively. Similarly, because *E. coli* was a key material for propelling hybrid micro/nanomotors, researchers used red blood cells (RBCs; erythrocytes) to construct bacteria-driven microswimmers that could be guided by bacteria *in vitro* [128]. RBCs loaded with the anticancer drug doxorubicin and superparamagnetic iron oxide NPs (SPIONs) were attached to bioengineered motile *E. coli* MG1655 through a biotin-avidin-biotin binding complex to form a multifunctional biohybrid microswimmer. The bacteria provided autonomous on-board propulsion to biohybrid microswimmers, and SPION-loaded RBCs enabled external magnetic navigation. In another study, the nonpathogenic MTB *Magnetospirillum gryphiswaldense* was combined with drug-loaded mesoporous silica microtubules to construct controllable microswimmers that could deliver antibiotics to infectious biofilms [129]. The movement of the hybrid organisms was also studied under the exogenous stimulation of a magnetic field. Vincenti *et al.* designed a rotary motor comprising living biological entities driven by an external alignment field [130]. At higher bacterial concentrations, interactions resulting from bacterial swimming activity in these regions formed a collective solid-like vortex flow in the central droplet core. To fabricate a similar hybrid structure, MTB had to accumulate in certain regions in a uniform magnetic field. The congregation of this active swimmer was limited by crowding, which led to instability that triggered coordinated movements at the droplet scale. Furthermore, the dependence of the active magnetic fluid on the original properties was the key, and the surrounding fluid was torqued by any swimming kinematics that changed the direction of the bacterial magnetic moment relative to that in an applied magnetic field.

2.4.3 Cardiomyocytes

The heart's pumping function is driven by the contractile force of myocardial engines, and muscle cells (cardiomyocytes) act through collective contractile activity [131]. In a previous study, researchers designed a polyacrylonitrile-based hydrogel yarn comprising uniaxially aligned nanofibers [132] and then implanted chicken cardiomyocytes in nanofiber hydrogel yarns to develop living cell-based microactuators. The devices maintained spontaneous cardiomyocyte pumping for 7 days. Shang *et al.* investigated an inverse opal exhibiting anisotropic periodic elliptical macropores and a hydrogel filling, stretch-derived for constructing and assembling tissues of biohybrid actuators (Figure 5C) [133]. The

researchers found that cultured cardiomyocytes induced into a highly ordered arrangement on the substrate surface could beat spontaneously and that spontaneous beating was recoverable. Cardiomyocyte beating was accompanied by cell contraction and elongation, and the synchronous cycle of deformation actuations that the anisotropic inverse opal can be observed as commensurate shifts in their photonic band gaps and structural hues. Cardiomyocyte-driven inverse opals offer the possibility for developing biohybrid actuators exhibiting self-driving capabilities. Inspired by the mechanism of structural color regulation in a chameleon, researchers developed a conceptually distinct structural color material by engineering the assembly of cardiomyocytes organized on a synthetic inverse opal hydrogel membrane exhibiting self-regulation ability [134]. During cardiomyocyte beating, cellular contraction and elongation caused the substrate membrane structure to exhibit a cycle of morphological and volumetric changes. Inspired by the crawling mechanism of caterpillars and the movement of snakes, Sun *et al.* developed a soft biological robot comprising asymmetric claws and carbon nanotube-induced myocardial tissue layers [135]. During cardiomyocyte contraction, the claws aided the directional movement. The directional conduction of the carbon nanotube layer adjusted the cardiomyocyte arrangement and improved the cardiomyocyte pulsatile and contractile properties. Cardiomyocyte-powered soft robots were excellent for simulating the caterpillar crawling behavior. In another study, researchers developed a tissue-engineered deformable robot that could assume different mechanical structures exhibiting different locomotive functions [136]. The robot was powered by a muscular caudal fin that mimics the swimming of a whale and functions as a cellular engine powered by synchronically contracting heart tissue structures. The system could be optically triggered to change from deployment to retraction, which effectively changed the bending stiffness of the tail to minimize, or even shut down, its propulsive output.

2.4.4 Insect dorsal vessels

Insect dorsal vascular (DV) tissue is environmentally stable and low maintenance, which make it ideal for application to microdrives. Akiyama *et al.* designed an insect muscle-powered autonomous microrobot (iPAM) driven by crustacean cardioactive peptides, which are neuroactive chemicals [137]. The robot comprised an artificial frame and DV tissue and moved quickly, which represents an elegant example of a biohybrid microdevice. For effectively utilizing the DV tissue contractile force to move the iPAM, the

molding frame was prepared based on a simulation using finite element analysis software. Moth larval DV tissues were assembled on the frame. Compared with the movement velocities of previously reported models, that of the current model considerably improved. The system exploited the spontaneous contraction of the insect DV tissue (DVT). Under culture conditions, DVT cells are more environmentally stable than mammalian tissues and cells. In another study, researchers developed a spontaneously moving polypod microrobot (PMR) by implementing DVT excised from an inchworm [138]. The researchers assembled the entire DVT on an inverted two-row array of micropillars to develop a prototype, which moved spontaneously at 3.5×10^{-2} $\mu\text{m/s}$, and the contractile force of the entire DVT was calculated at 20 μN . From the prototype, they produced a real PMR, which exhibited considerably enhanced velocity and spontaneously moved at 3.5 $\mu\text{m/s}$. Uesugi *et al.* developed a bioactuator that exhibited contractile properties and controllability [139]. The bioactuator was fabricated using the DVT of an insect (final-stage moth larva) and different stimulation strategies. The high robustness of the insect tissue produced an excellent biological actuator.

2.4.5 Skeletal muscle cells

Skeletal muscles can generate stronger contractile forces than cardiomyocytes. Typical skeletal muscle cells can generate a force as strong as 400 μN [140]. In animals, skeletal muscle is the primary actuator, which is the interface between neurons and bones. Owing to their modular structure, these muscles generate enormous contractile forces in rapid succession upon receiving signals from motor neurons. Skeletal muscles can be a key material for propelling micro/nanomotors and developing biohybrid robots [141]. In all animals, pumps are critical parts. During the first moments of life, the tubular embryonic heart functions as a valveless pump, which generates unidirectional blood flow. After studying this basic pump, researchers designed a biohybrid valveless pump robot powered by engineered skeletal muscle [142]. This pump robot comprised a soft hydrogel tube attached at both ends to a stiffer polydimethylsiloxane scaffold, which generated an impedance mismatch. A ring of contractile muscle tissue wrapped the hydrogel tube off-center and squeezed the tube with or without local buckling. Cyclic muscular contractions, electrically stimulated or spontaneous, further squeezed the tube, causing elastic waves to propagate along the hose and reflect back at the soft/hard tube boundary. The asymmetric placement of the muscle ring generates a

wave-to-wave time delay that establishes a net unidirectional flow regardless of whether the tube is buckled. Presently, pump-bots can achieve flow rates of up to 22.5 $\mu\text{L/min}$. In animals, skeletal muscle cells are the main actuating factors and, with appropriate optogenetic modification, can be adjusted using electromagnetic or electric fields. Hasebe *et al.* designed a synthetic powerplant (**Figure 5D**) comprising microgrooved membranes powered by aligned contractile skeletal muscle cells [143]. To develop the system, a thermoplastic elastomer comprising poly(styrene-*block*-butadiene-*block*-styrene) (SBS) was prepared. Because SBS thin films are easy to handle and fabricate and exhibit low flexural rigidity, they have attracted considerable research attention for application to flexible substrates that can be used for designing advanced biohybrid actuators that can deform when cells shrink. SBS thin films are an interesting candidate scaffold for developing biohybrid drives. Aydin *et al.* developed a biohybrid swimmer powered by an on-board neuromuscular unit [144]. The swimmer's body comprised skeletal muscle tissue, independent soft scaffolds, and motor neuron-containing optogenetic stem cell-derived neural clusters. However, this sensory-motor pattern depended on the ability of neural units to direct muscle movement. Periodic muscle contractions generated by nerve stimulations drove the time-irreversible flagellar dynamics, which provided the driving force required for moving the micro/nanomotor tether forward.

Biohybrid microswimmers can have a pivotal impact on both tissue engineering and bionics [145]. Cell-like micro/nanomotors (which can be categorized as cell-based and cell membrane-coated motors) have recently shown great progress. Cell-like micro/nanomotors, for which drivers exhibit biological components (e.g., bacteria or sperm drivers); synthetic micro/nanomotors (e.g., fuel-free actuation or chemical self-propulsion); or cellular micro/nanomotors (e.g., entire cells or cell membranes) can prevent biological contamination and facilitate micro/nanomotor propulsion in complex biological fluids, such as blood. Compared with static motors, cell-like micro/nanomotors can exhibit faster biological detoxification by designing and combining the dynamic motion characteristics of synthetic motors with the multifunctionality of cellular components and facilitate disease-targeted drug delivery. The integration and assembly of cell materials and artificial micro/nanomotor structures improve and prolong the actuation of biological fluids, drug loadings and releases, and localization and targeting of imaging and therapeutic drugs. Although these cell-like micro/nanomotors exhibit unique advan-

tages, some important challenges remain for potentially applying such micro/nanomotors *in vivo*. These include the further development of improved propulsion in rich and complex biological fluids; collective propulsion to control the motor velocity and direction; comprehensive biocompatible size, design, and function; enhanced tissue retention in therapeutic and imaging applications; and abilities to eliminate residues through self-decomposition and consume toxic fuels (e.g., H_2O_2). To achieve long-term propulsion in blood, which is an important challenge in the application of micro/nanomotors, the cellular components must remain intact. Other cellular motors exhibiting intrinsic chemotactic behavior, such as sperm and bacteria, can be used for sensing and responding to chemoattractants and targeting cargo delivery *in vivo*. Furthermore, to apply cellular motors, such as bacteria, to organisms foreign to the host, attention must be exercised to prevent immune responses and infection [7]. Sperm cells are a suitable candidate for working in physiological environments because sperm do not contain disease-causing proteins or multiply to proliferate colonies as other cells or microbes do. Bacterial biohybrids comprise self-propelled bacteria carrying micro/nanomaterials and can transport their payload to a specified location under exogenous stimulation conditions, which potentially opens avenues in minimally invasive medicine [146]. Sperm-mixing micro/nanomotors exhibit good biocompatibility and potential applications in gynecological treatments, healthcare, and the detection of cancer or other diseases of the female reproductive system. However, sperm-mixing micro/nanomotors exhibit a short working life because living sperm cells are particularly prone to inactivation. Therefore, more research is required to develop cells that can replace sperm. Bacteria-driven microswimmers are multifunctional and high-performance micro/nanomotors. Bacteria can combine with synthetic substances to perform various functions. The translation of bacterial-driven microswimmers into cargo delivery and clinical diagnostic devices requires the conception and preparation of versatile cargo carriers exhibiting excellent properties, such as biocompatibility, payload efficiency, stability, biodegradability, and deformability [128]. Cardiomyocyte beating is accompanied by cellular contraction and elongation, and cardiomyocytes exhibit pumping behavior in native myocardium tissue. Cardiomyocytes, insect DVT, and skeletal muscle cells all exhibit pumping behavior. Therefore, materials derived from these cells are inherently biocompatible, and micro/nanomotors synthesized from these cells do not elicit immune responses. Finally, autonomously moving cell-driven biohybrid motors

would enable a built-in chemotactic motion, which avoids reliance on complex actuation equipment or harmful fuels [7].

3. Applications

The complex environment in which micro/nanomotors are positioned, primarily referring to endogenous and exogenous stimuli, cannot be isolated from the driving and application of micro/nanomotors. Endogenous substances more frequently include water [34], urine [35], glucose [36], and hydrogen peroxide [37, 38]. In response to endogenous stimuli, micro/nanomotors produce a propulsion gradient. Micro/nanomotors can be used to propel living cells and biological organisms because water and hydrogen peroxide are relatively prevalent endogenous components in living organisms. One of the endogenous stimuli can function as both a micro/nanomotor driver and potential therapeutic agent. For instance, while driving the micro/nanomotors through redox interactions with essential components, endogenous stimuli can correct or improve hypoxic deficiencies in tumor microenvironments, which is crucial for implementing photodynamic therapy in cancer treatment. Optical [24–27], magnetic [28–30], auditory [31, 32], and electric [33] fields are other common external stimuli. Propulsion can be accomplished using magnetic fields, which can accurately modulate micro/nanomotors through the involvement and management of exogenous stimuli. This is possible because most materials of power devices fabricated using micro/nanomotors are magnetic substances [74].

In biomedical disciplines, self-propulsion micro/nanomotors are essential [147]. Nanomotors exhibit different morphologies [148] and motion mechanisms [149, 150] and are fabricated using materials [151, 152] exhibiting different biocompatibilities [153–155]. Owing to important advances over the past few decades, micro/nanorobots can efficiently navigate to target destinations in physiological environments by converting various energies to kinetic energy and attaining propulsion. According to previous studies, micro/nanomotors offer a wide range of applications, including the direct loading, transport, and delivery of therapeutic payloads to disease locations, which minimizes detrimental effects on organisms and enhances therapeutic results [13]. Numerous facets of life, including biosensing and disease treatment, are impacted by employing nanomotors.

3.1 Biosensing

The trapping agent on the micro/nanomotor surface captures and detects environmental substances with a power device. Janus particles are

frequently used in self-propelled optical nanoprobe, biosensors, and micro/nanomotors [156, 157]. Micro/nanomotors efficiently detect mainly nucleic acids (DNA and RNA) [158, 159], cancer cells [160], bacteria [161], hormones [162], and proteins (such as pepsinogen [163], lysozymes [164], immunoglobulins [165], and cholesterol [166]).

Because of their enormous potential in actuation systems and smart sensing, micro/nanomotors and

biosensors show potential as effective tools for administering medication and for early diagnosis in precision medicine. Micro/nanomotors and biosensors exhibiting good biocompatibility have been constructed by optically binding living RBCs to waveguides with fiberoptic probes. Additionally, blood pH has been measured by monitoring the RBC waveguide's light transmission, which could help diagnose pH-related blood diseases [17].

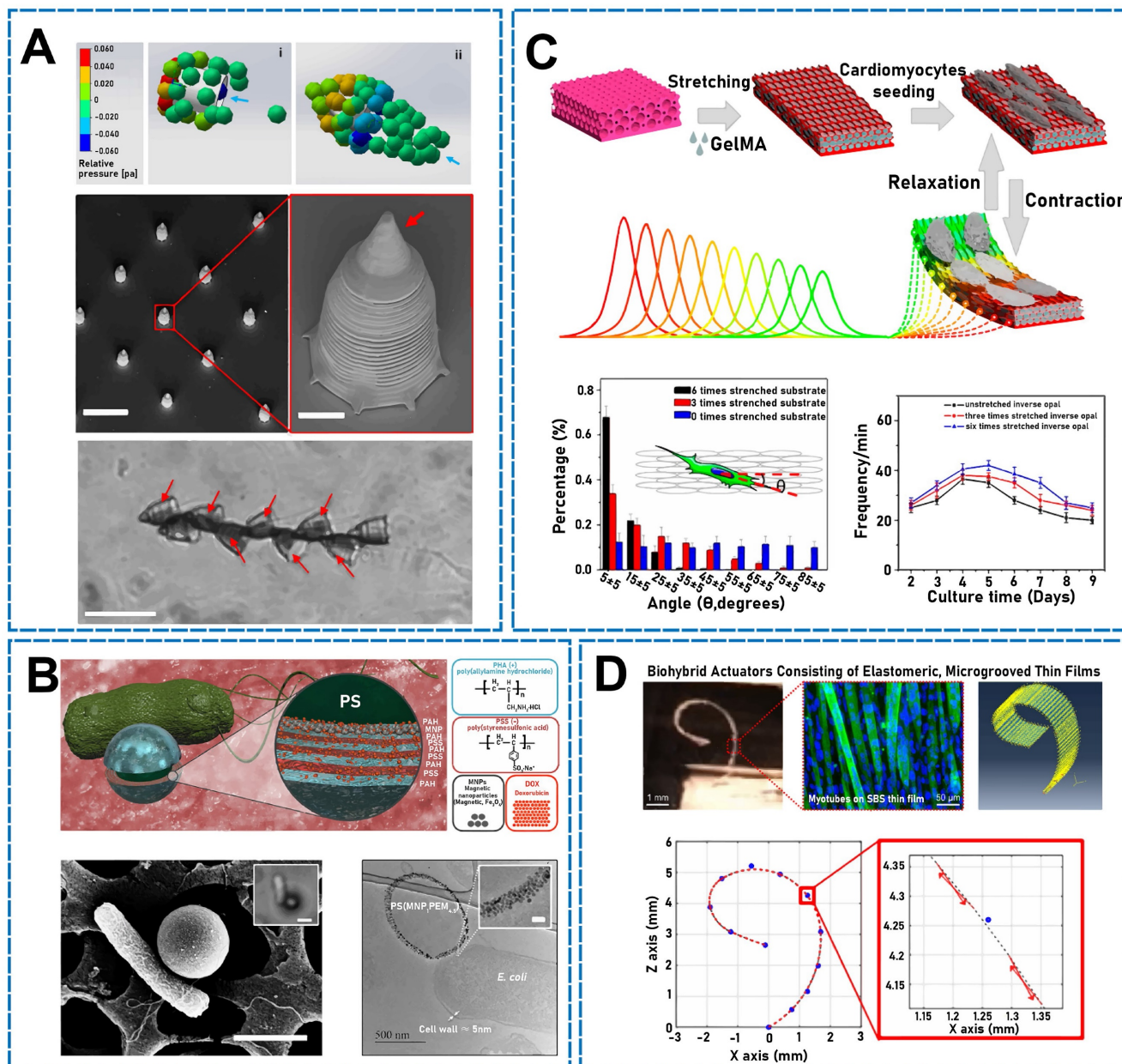


Figure 5. (A) Hydrodynamic simulations of the model. SEM images of streamlined-horned caps. Sperm train swimming in sperm medium. Reproduced with permission [123]. Copyright 2020, American Chemical Society. (B) The design of multifunctional bacteria-driven microswimmers. SEM image of a single PS (MNP;PAH/PSS) +PAH-attached cell. TEM image of a microswimmers thin section. Reproduced with permission [125]. Copyright 2017, American Chemical Society. (C) Synthesis of the biohybrid actuator. Cardiomyocytes drive corresponding color changes in substrates structures. Orientation angle frequency distribution of cardiomyocytes. The beating properties of cardiomyocytes. Reproduced with permission [133]. Copyright 2019, American Chemical Society. (D) Biohybrid machine model. Finite element model simulation setting and results. Reproduced with permission [143]. Copyright 2019, American Chemical Society.

To mimic the mobility of planktonic jellyfish, Zhang *et al.* developed a micro/nanomotor comprising a multimetallic shell and catalase-modified DNA component [158]. The jellyfish-resembling micro/nanomotor was propelled by the peroxidase's catalytic decomposition of H_2O_2 to generate oxygen. The open sensing surface of this micro/nanomotor effectively recognized the target molecule to detect DNA motion accurately and sensitively, which considerably benefits DNA detection. In addition, the micro/nanomotor is simple to prepare, exhibits good motion performance, and sensitively detects DNA motion. A class of endogenous small-molecule RNAs, known as miRNAs, plays a crucial role in cell differentiation, value addition, and death. The Janus mesoporous microsphere/Pt-based (meso-MS/Pt) nanostructure developed by Zhang *et al.* (**Figure 6A**) considerably improved target delivery and accelerated recognition for miRNA amplification and detection in intricate biological samples [159]. Meso-MS/Pt/DNA micro/nanomotors have been demonstrated as a more creative concept and technique for analyzing miRNAs in authentic biological materials.

Procalcitonin (PCT) is an indicator used to determine the presence of bacterial infections. Calcitoninogen is a hormone generated by the human endocrine system to regulate calcium and phosphorus metabolism and lowers blood calcium levels for surveilling infectious diseases. To evaluate PCT and identify early sepsis, researchers have developed a fluorescence micromotor-based immunoassay (FMIm) (**Figure 6B**) [161]. The micromotor actively recognizes PCT antigens based on magnetic guiding (Ni layer), the catalytic generation of oxygen bubbles (PtNP inner layer), and the high binding capacity of particular antibodies adapted to the polymeric polypyrrole outer layer. This FMIm enables the detection of an extremely low content (25 μ L) in a clinically relevant concentration range (0.5–150 ng/mL) and direct PCT detection in clinical samples from very-low-birthweight infants suspected of having sepsis (LOD = 0.07 ng/mL).

Using a bispecific aptamer initiator, DNAzyme, and an entropy-driven circuit that uses rolling and walking motions to maximize signal amplification, Qi *et al.* developed a 3D DNA nanomotion biosensor for sensitively and specifically detecting lysozymes [164]. Owing to the strong selectivity of the bispecific aptamer, the 3D DNA nanomotor biosensor may react to lysozymes with high specificity and quickly release the signal. Because the entire procedure is protease-independent, the operational stability is not affected by unfavorable environmental conditions. The lysozyme detection threshold was as low as

0.01 pg/mL in the linear range from 0.05 pg to 500 ng/mL. In addition, this strategy was highly accurate for analyzing samples, indicating the excellent application potential of the nanomotion biosensor for detecting nonnucleic acid targets.

To develop ultrasmall enzyme/photovoltaic nanomotors for detecting cholesterol, researchers prepared ultrasmall histidine-modified Fe_3O_4 NPs ($UHFe_3O_4$ NPs) that were connected directly with cholesterol oxidase (ChOx) [166]. As a chemical catalyst, ChOx uses cholesterol oxidation to initiate $UHFe_3O_4@ChOx$ and generate H_2O_2 . $UHFe_3O_4$ NPs function as nanoenzymes to catalyze the subsequent color development reaction between H_2O_2 and 3,3',5,5'-tetramethylbenzidine for detecting cholesterol while simultaneously functioning as a photothermal engine powering NIR light. These NPs exhibit both the peroxidase-mimetic property and photothermal effects. In the linear response range of 2–100 μ M, $UHFe_3O_4@ChOx$ functioned as a cholesterol sensor, which increased the sensitivity, accelerated the analysis, and detected cholesterol concentrations as low as 0.178 μ M.

For accurate biological sampling, precision medicine to diagnose illnesses, and controlled delivery of medications, the various strategies of contemporary micro/nanomotor platforms offer a more practical method to ensure human life and health [167].

3.2 Disease treatment

In relation to human health, cancer remains a major challenge [168]. The micro/nanomotor and power unit sizes enable the enhanced penetration of micro/nanomotors in sexual organs and therapeutic tissues, which provides micro/nanomotors with a wide range of application prospects in disease treatment. Nanomotors can be applied to treat malignant tumors [169, 170, 171], gynecological cancer [121], gastric ulcers [172], and atherosclerosis (AS) [173]; capture and transport fertilized oocytes [174]; eradicate fungal infections [175]; treat bladder cancer [176]; modulate the immune system [177]; and repair damaged tissues [178, 179], and enhance bioadhesion and tissues penetration of biomedicine [180], all of which are extraordinarily important. Nanomotors can achieve these remarkable medical functionalities because they can provide targeted drug delivery [181,182] related to their driving mechanism and key materials.

To enhance synergistic antifungal therapy for transdermal delivery, researchers have designed a parachute-like nanomotor loaded with miconazole nitrate (PNM-MN) propelled under NIR irradiation [175]. Owing to the distribution asymmetry in the

PNM space, effective self-thermophoretic propulsion was achieved after the generation of a thermal gradient under NIR laser irradiation. The photothermal effect and pharmacological therapy of PNM can obliterate *Candida albicans* and biofilms, respectively. Furthermore, the drug uses nanomotors and NIR laser irradiation to penetrate the skin and reach the infection site effectively. Because the cellular membrane defends the cytoplasm, the delivery of extracellular drugs to cells is difficult, which limits their application to disease treatment. This encourages the application of self-propelled micro/nanomotors as carriers of orally administered drugs for treating gastrointestinal diseases. Researchers have developed a bioinspired, enzyme-driven biopolymeric micro/nanomotor that replicates the ability of *Helicobacter pylori* to penetrate stomach

mucus [183]. In acidic environments, immobilized urease effectively converts urea to ammonia, and the resultant increasing pH changes the local mucin layer from a gel to a sol, which aids the penetration of the gastric tissue layer. According to the study findings, the micro/nanomotors were eliminated from the body within 3 days without negatively affecting the digestive system. The enhanced penetration and retention of micro/nanomotors as an active oral delivery vehicle in the stomach will be used for treating various gastrointestinal disorders.

In another study, an NO-driven nanomotor was constructed in a tumor microenvironment [184]. During the movement, NO was released and played an important role in regulating the infiltration activity and behavior of T cells in the tumor microenvironment. The micro/nanomotor was accom-

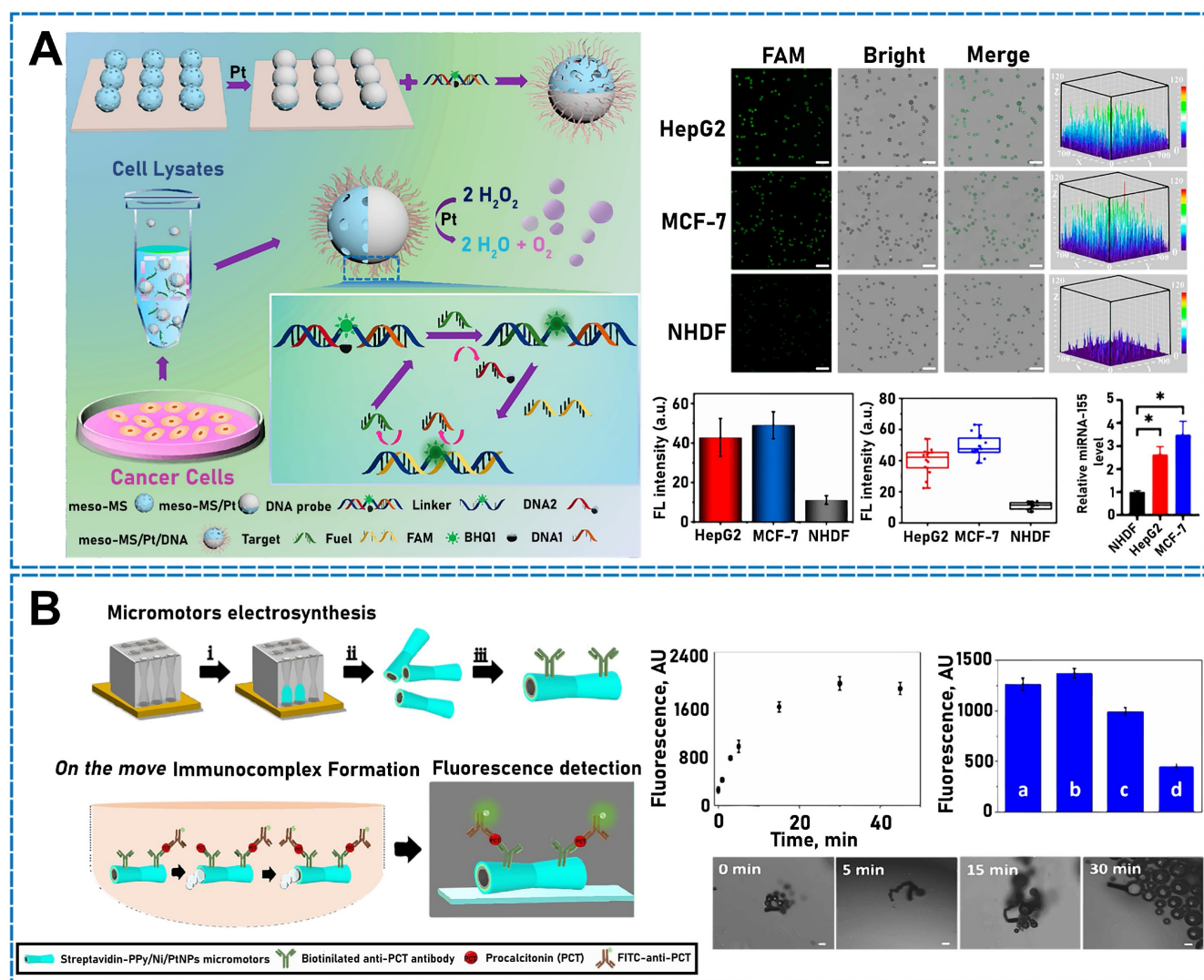


Figure 6. (A) Schematic diagram of Meso-MS/Pt/DNA micro/nanomotor for *in vitro* miRNA detection. Meso-MS/Pt/DNA CLSM images. FL intensity in NHDF, HepG2, and MCF-7 cell lysates. Relative miRNA-155 levels of NHDF, HepG2, and MCF-7 cells. Reproduced with permission [159]. Copyright 2022, American Chemical Society. (B) Schematic diagram of the synthesis of anti-PCT-PPy/Ni/PtNP micromotor. Determination of PCT by FIM method. Effect of time on fluorescence signal and time-lapse images of the micromotor in plasma samples. Performance of immunoassay under different driving conditions. Reproduced with permission [161]. Copyright 2020, American Chemical Society.

panied by the release of NO during propulsion. The regulation of the tumor microenvironment by NO-driven nanomotors enabled the simultaneous deep penetration of microscale T cells and nanoscale drugs. Moreover, for simultaneous molecular imaging with spatiotemporal resolution, drug administration, and multifunctional cell targeting, Park *et al.* developed a mesoporous silica nanosphere exhibiting an optical nanocrescent antenna [185]. This molecule was light driven, which enabled the rapid apoptosis of breast cancer cells through the delivery of doxorubicin. The excellent permeability of the power unit and micro/nanomotors make them promising candidates for delivering drugs and deeply treating malignant tumors. Li *et al.* developed an H₂O₂-propelled Janus gold nanorod–platinum (J AuNR–Pt) nanomotor (**Figure 7**) [186] for application to photoacoustic imaging in the second NIR region (NIR-II) of deep tumor tissues and effectively treated tumors with excellent detection and therapeutic integration. The J AuNR–Pt nanomotor driver enhanced the cellular uptake of the drug and improved the lysosomal escape, which was more conducive to the sustained release of cytotoxic Pt²⁺ ions in the nucleus to damage DNA and stimulate tumor cell apoptosis. The results suggested that the J AuNR–Pt nanomotor deeply penetrated, accumulated in, and treated tumors effectively.

Because sperm cells are naturally optimized to swim in the female reproductive system, they can be applied for treating cervical cancer and other gynecological diseases. Therefore, Xu *et al.* developed a drug delivery system based on sperm-hybrid micro/nanomotors [121]. In this bionic micro/nanomotor, sperm naturally swim to tumor lesions and fuse with somatic cells therein, which enables them to function as drug carriers for potentially treating cancers in the female reproductive tract by effectively transferring drugs to target cells/tumors. In addition, sperm cells function as a propulsion source, while the magnetic microstructure is used to guide and release sperm. The microstructural arm bends as it contacts the cell, which generates a pathway for releasing sperm. This sperm-hybrid micro/nanomotor exhibits excellent biocompatibility and has potential for application to gynecological care and the treatment and detection of cancer and other diseases in the female reproductive system.

Currently, several drugs exhibit low efficacy for treating bacterial infections, which have become multidrug-resistant. This has broadened the scope of bacterial infections and, therefore, endangers human health. To solve this problem, researchers have designed nanomotors [187] comprising urease-, lysozyme-, and urease- and lysozyme-functionalized

MSNPs (U-MSNPs, L-MSNPs, and M-MSNPs, respectively) exhibiting antibacterial properties against nonpathogenic planktonic *E. coli*. Urease catalyzed the urea generation of NaHCO₃, NH₃ drove the micro/nanomotors, and U-MSNPs exhibited the highest bactericidal activity. Above 200 µg/mL, U-MSNPs reduced the biofilm biomass of uropathogenic *E. coli* by 60%. These results demonstrated the ability of functionalized enzymatic micro/nanomotors to fight infectious diseases.

Traditional methods for treating AS involve surgical and pharmaceutical interventions. However, these methods are invasive and cause various side effects. Owing to the micro/nanomotor's permeability and drug delivery capability, considerable progress has been made in alternative methods for treating AS. Wu *et al.* developed a driver for alginate (Tr, one of the mTOR-independent autophagy inducers), L-arginine (Arg), and phosphatidylserine (PS) (**Figure 8**) [188]. At AS sites, ROS and inducible nitric oxide synthase (iNOS) were highly expressed and functioned as agents for inducing the chemotactic behavior of micro/nanomotors, which is the first step in targeting AS plaques. Then, corresponding PS signals were used to target macrophages in AS plaques gradually and precisely. During the treatment, ROS regulated the M2 polarization of macrophages, and NO contributed to the reconstruction of the endothelial barrier, which can treat AS in a multilinked manner.

We have highlighted the “smart” behaviors of micro/nanomotors for various fantastic biomedical applications [189]. Owing to their ability to distribute medications, treat various ailments, and investigate intricate biological microenvironments without using any external cells, nanomotors are obviously indispensable.

4. Conclusions and perspectives

To date, micro/nanomotors have shown excellent promise in disease treatment and biosensing applications. Metals or compounds being not the only key materials available for driving micro/nanomotors, biocompatible, environmentally friendly, and biodegradable “biosmart” micro/nanomotors have been developed by combining various preparation techniques and continuously exploring key materials for driving micro/nanomotors. Enzymes, which are abundant in living organisms and transform chemical into mechanical energy, are another example of a key material. Biocompatible and biodegradable micro/nanomotors can be produced using enzymes as biocatalysts to provide the energy required to drive such motors. Owing to their natural propulsion or contractility, spermatozoa, cardiac skeletal muscle,

and insect dorsal blood arteries can all be employed as “pumps” for biohybrid micro/nanomotors. In addition to exhibiting well-controlled deformability, micro/nanomotors can reduce biological contamination and facilitate micro/nanomotor movement through complex biological fluids, such as blood. The investigation of these drivers may suggest further avenues for applying micro/nanomotors.

Because several important and intriguing studies

support the application expansion of micro/nanomotors, a more thorough overview is required because, to the best of our knowledge, no research is currently available in the literature on the classification of micro/nanomotors according to different material types, endogenous substances, and exogenous stimuli, especially for micro/nanomotors powered by cardiomyocytes, insect dorsal vessels, and skeletal muscle cells. Additionally, our in-depth

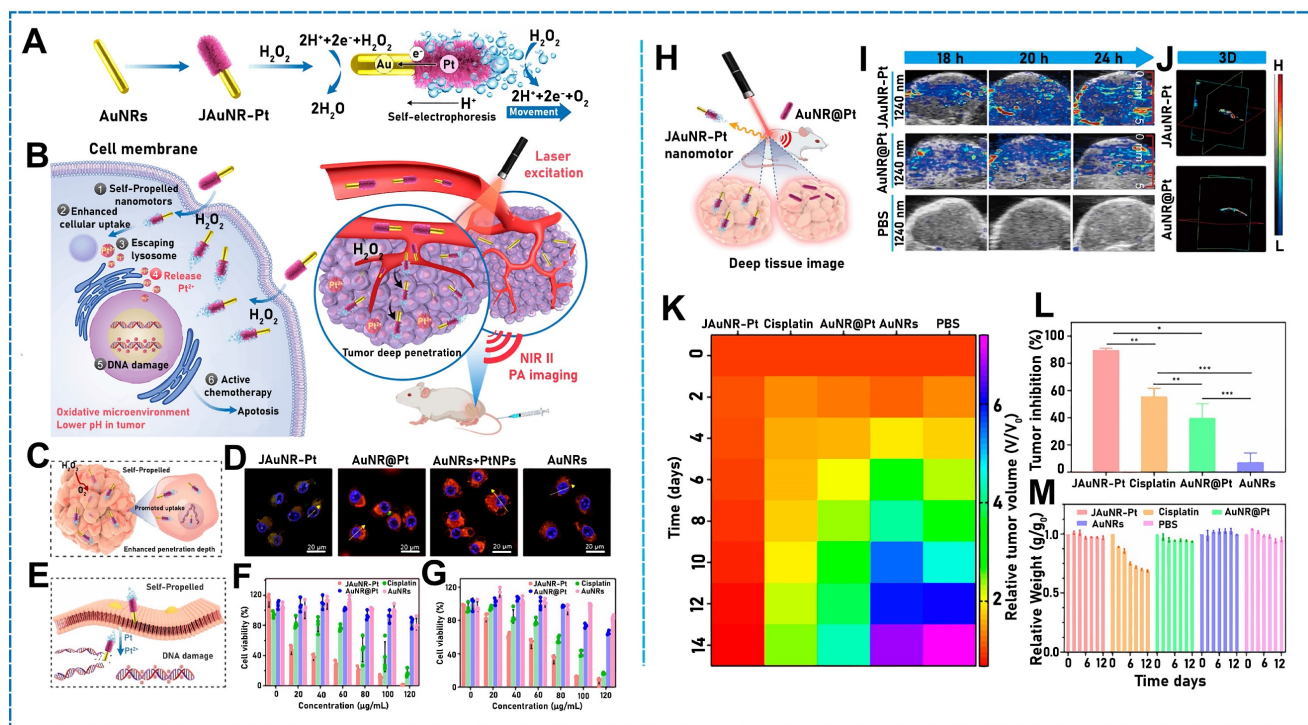


Figure 7. (A) Schematic diagram of the synthesis of JAuNR-Pt nanomotor. (B) JAuNR-Pt nanomotor for cancer therapy. (C) Schematic diagram of the permeability mechanism of the nanomotor. (D) Colocalization of nanomotors with the nucleus and lysosomal tracker. (E) Schematic diagram of cell treatment with JAuNR-Pt nanomotors. (F) - (G) Cell viabilities. (H) Schematic diagram of nanomotor permeability *in vivo*. (I) Photoacoustic (PA) image of *in vivo* tumor injected with JAuNR-Pt nanomotor. (J) 3D PA image of *in vivo* tumor. (K) Changes in tumor volume after *in vivo* antitumor. (L) Tumor inhibition. (M) Weight changes of mice in different treatment groups. Reproduced with permission [186]. Copyright 2022, American Chemical Society.

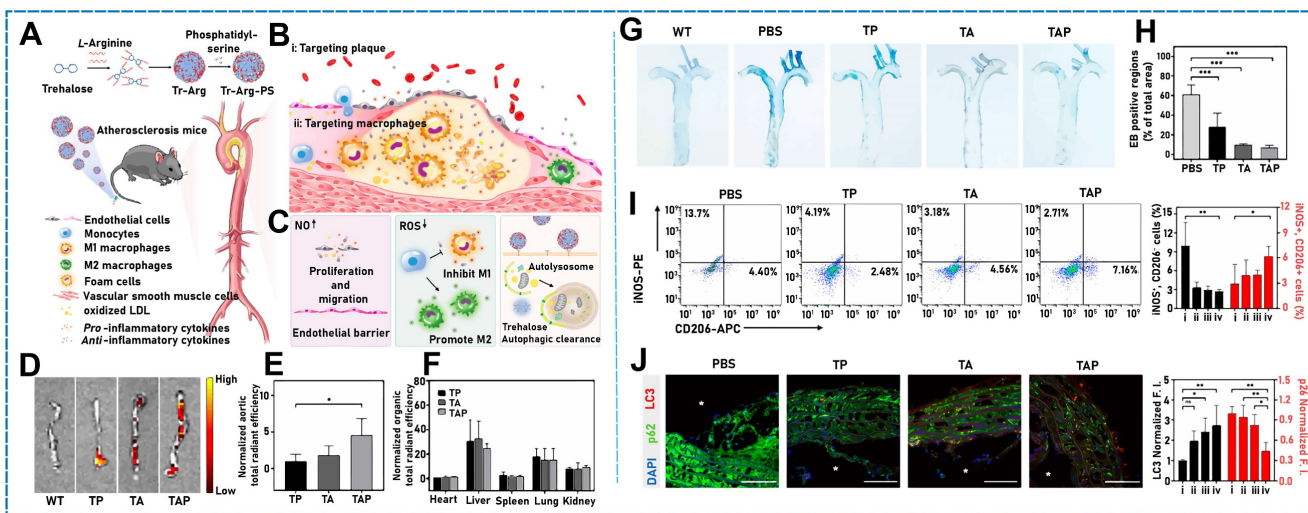


Figure 8. (A) Preparation process of TAP nanomotors. (B) Targeting mechanism of TAP nanomotors. (C) Integrated anti-atherosclerotic effect of TAP nanomotors. (D)-(F) Capacity to target plaque-associated macrophages *in vivo* and anti-atherosclerotic response. (G) Aortic staining of atherosclerotic mice with different sample treatments. (H) Quantitative analysis. (I) Analysis of macrophage subsets by flow cytometry in the aortas of mice with atherosclerosis. (J) Autophagy-related proteins are seen in cryosections of the aortic arch in immunofluorescence pictures. Reproduced with permission [188]. Copyright 2022, American Chemical Society.

analysis of micro/nanomotors may bring readers up to date on the development of these interdisciplinary fields, which include chemistry, biology, nanomedicine, and materials research. Because micro/nanomotor research is a multidisciplinary field, the limitations of micro/nanomotors will be overcome, which will improve the practical application prospects of micro/nanomotors.

In this review, we have summarized the main components powering micro/nanomotors and examined the effects of endogenous compounds and external stimuli on micro/nanomotor movement. We also explored the application of micro/nanomotors for biosensing and treating diseases. Because they are tiny in liquid environments, micro/nanomotors cannot overcome Brownian motion, which hinders the generation of more ideal directional motion, and different resistances in complex environments are some of the main drawbacks of micro/nanomotors. Additionally, whether micro/nanomotors can meet all the challenges for developing desirable practical applications remains unclear. However, compared with conventional nanomedicines, micro/nanomotors face numerous challenges related to shorter lifespans, more difficult preparation techniques, high costs, and potentially unfavorable biocompatibilities. Currently, micro/nanomotors may be superior to conventional nanomedicines for treating malignant diseases. Compared with conventional nanomedicines, micro/nanomotor power devices may effectively, rapidly, and completely detect and decompose targets in real time and be recycled and reused. All these characteristics endow micro/nanomotors with excellent application potential. To improve therapeutic outcomes, micro/nanomotors should boost synergistic treatments, deeply penetrate targeted tissues, effectively decompose targets, and mitigate the negative effects of extremely toxic medications.

The utilization of these essential materials to drive micro/nanomotors for sensing detection, illness treatment, and other intriguing applications must still be developed further and should be thoroughly evaluated in practical and clinical applications. The key components that power micro/nanomotors are currently being intensively studied and analyzed in a wide range of applications. The application potential of biosensing, which should provide insights for transmitting biosignals, is unquestionably beneficial for improving health. In the meantime, potential micro/nanomotor applications extend beyond sensing and detection and include the treatment of severe illnesses. Micro/nanomotors enable synergistic hydrogen chemotherapy and drug delivery for treating cancer and have considerable promise for numerous biomedical applications, including

platforms and methods for treating various malignancies.

Abbreviations

- ALG: Alginate
- AMB: Magnetospirillum magneticum AMB-1
- AS: atherosclerosis
- BiOI: bismuth oxyiodide
- BNN6: N, N-di-sec-butyl-N, N-dinitroso-1,4-phenylenediamine
- B@P@C: BNN6@PDA@CREKA
- CAT: catalase
- CCMP: calcium carbonate microparticle
- CHI: chitosan
- CNF: carbonaceous nanoflake
- CREKA: Cys-Arg-Glu-Lys-Ala
- Cu₂O@GO: cuprous oxide @ graphene oxide
- CXCL12: chemokine (C-X-C motif) ligand 12
- D: Diameter
- DV: dorsal vascular
- DVT: dorsal vascular tissue
- E-H-motor: emulsion hydrogel motor
- EMNM: enzyme-powered micro/nanomotors
- Fe-BTC: Iron 1,3,5-benzenetricarboxylate
- FSFSMs: free swimming functionalized sperm micromotors
- GO: graphene oxide
- GOx: glucose oxidase
- hQN: hairpin DNA quadrilateral nanostructure
- ID: inner diameter
- iNOS: inducible nitric oxide synthase
- iPAM: insect muscle-powered autonomous microrobot
- JMs: Janus micromotors
- JMSNM: Janus mesoporous silica nanomotor
- JRs: Janus rods
- JUS motors: Janus upconversion nanoparticle-SiO₂ micromotors
- KF: kapok fiber
- L: Length
- LbL: layer-by-layer
- L-MSNPs: MSNPs functionalized with lysozyme
- LOD: limit of detection
- meso-MS/Pt: mesoporous microsphere/Pt-based
- miRNAs: microRNAs
- M-MSNPs: MSNPs functionalized with urease and lysozyme
- MNPs: magnetic nanoparticles
- MOFs: metal organic frameworks
- MOFtors: MOF motors
- MSNP: mesoporous silica nanoparticle
- MTB: magnetotactic bacteria
- MΦ: Macrophage
- NIR: near-infrared

NOS: NO synthase
 NPs: Nanoparticles
 PAzoMA: poly [6-(4-methoxy-4 -oxyazobenzene) hexyl methacrylate
 PCT: Procalcitonin
 PDA: polydopamine
 PEDOT: poly(3,4-ethylenedioxythiophene)
 PEDOT-PSS/Au: poly (3,4-ethylenedioxythiophene and sodium 4-styrenesulfonate)/ Au microtube
 PLGA: polylactic-glycolic acid
 PMR: polypod microrobot
 PPyNP: poly pyrrole nanoparticle
 PS: phosphatidylserine
 PSS: poly (sodium 4-styrenesulfonate)
 PVA: poly (vinyl alcohol)
 RBCs: red blood cells
 RGO: reduced graphene oxide
 ROS: reactive oxygen species
 SAMTB: semi-artificial magnetotactic bacteria
 SPION: superparamagnetic iron oxide nanoparticle
 THK: thickness
 3D: three-dimensional
 UHF₃O₄ NPs: ultrasmall histidine-modified Fe₃O₄ nanoparticles
 U-MSNPs: MSNPs functionalized with urease

Acknowledgements

This work was supported by the National Natural Science Foundation of China (22276102), the Young Taishan Scholars Program of Shandong Province of China (tsqn202211212), the Shandong Provincial Natural Science Foundation (ZR2022MB024), the University Institute Innovation Team of Jinan (202228027), and the 2022 Science, Education and Industry Integration Pilot Project Plan of Qilu University of Technology (Shandong Academy of Sciences) (2022PT114).

Competing Interests

The authors have declared that no competing interest exists.

References

- Zheng J, Qi R, Dai C, Li G, Sang M. Enzyme catalysis biomotor engineering of neutrophils for nanodrug delivery and cell-based thrombolytic therapy. *ACS Nano*. 2022; 16: 2330-44.
- Wang L, Liu Y, He J, Hourwitz MJ, Yang Y, Fourkas JT, et al. Continuous microfluidic self-assembly of hybrid Janus-like vesicular motors: Autonomous propulsion and controlled release. *Small*. 2015; 11: 3762-7.
- Boehnke N, Straehla JP, Safford HC, Kocak M, Rees MG, Ronan M, et al. Massively parallel pooled screening reveals genomic determinants of nanoparticle delivery. *Science*. 2022; 377: eabm5551.
- Serrà A, García-Torres J. Electrochemistry: A basic and powerful tool for micro-and nanomotor fabrication and characterization. *Appl Mater Today*. 2021; 22: 100939.
- Lyu X, Liu X, Zhou C, Duan S, Xu P, Dai J, et al. Active, yet little mobility: Asymmetric decomposition of H₂O₂ is not sufficient in propelling catalytic micromotors. *J Am Chem Soc*. 2021; 143: 12154-64.
- Arque X, Andres X, Mestre R, Ciraulo B, Ortega Arroyo J, Quidant R, et al. Ionic species affect the self-propulsion of urease-powered micromotors. *Research*. 2020; 2020: 2424972.
- Esteban-Fernandez de Avila B, Gao W, Karshalev E, Zhang L, Wang J. Cell-like micromotors. *Acc Chem Res*. 2018; 51: 1901-10.
- Ren M, Guo W, Guo H, Ren X. Microfluidic fabrication of bubble-propelled micromotors for wastewater treatment. *ACS Appl Mater Interfaces*. 2019; 11: 22761-7.
- Rayaroth MP, Oh D, Lee CS, Kumari N, Lee IS, Chang YS. Carbon-nitride-based micromotor driven by chromate-hydrogen peroxide redox system: Application for removal of sulfamethaxazole. *J Colloid Interface Sci*. 2021; 597: 94-103.
- Ye H, Sun H, Wang S. Electrochemical synthesis of graphene/MnO₂ in an architecture of bilayer microtubes as micromotors. *Chem Eng J*. 2017; 324: 251-8.
- Kim K, Guo J, Liang Z, Fan D. Artificial micro/nanomachines for bioapplications: biochemical delivery and diagnostic sensing. *Adv Funct Mater*. 2018; 28: 1705867.
- Maric T, Nasir MZM, Rosli NF, Budanović M, Webster RD, Cho NJ, et al. Microrobots derived from variety plant pollen grains for efficient environmental clean up and as an anti-cancer drug carrier. *Adv Funct Mater*. 2020; 30: 2000112.
- Luo M, Feng Y, Wang T, Guan J. Micro-/nanorobots at work in active drug delivery. *Adv Funct Mater*. 2018; 28: 1706100.
- Diez P, Lucena-Sanchez E, Escudero A, Llopis-Lorente A, Villalonga R, Martínez-Manez R. Ultrafast directional Janus Pt-mesoporous silica nanomotors for smart drug delivery. *ACS Nano*. 2021; 15: 4467-80.
- Wang D, Gao C, Zhou C, Lin Z, He Q. Leukocyte membrane-coated liquid metal nanoswimmers for actively targeted delivery and synergistic chemophotothermal therapy. *Research*. 2020; 2020: 3676954.
- Dong R, Hu Y, Wu Y, Gao W, Ren B, Wang Q, et al. Visible-light-driven BiOI-based Janus micromotor in pure water. *J Am Chem Soc*. 2017; 139: 1722-5.
- Li Y, Liu X, Xu X, Xin H, Zhang Y, Li B. Red-blood-cell waveguide as a living biosensor and micromotor. *Adv Funct Mater*. 2019; 29: 1905568.
- Wu X, Ehehalt R, Razinskas G, Feichtner T, Qin J, Hecht B. Light-driven microdrones. *Nat Nanotechnol*. 2022; 17: 477-84.
- Zou X, Zheng Q, Wu D, Lei H. Controllable cellular micromotors based on optical tweezers. *Adv Funct Mater*. 2020; 30: 2002081.
- Chen B, Liu L, Liu K, Tong F, Wang S, Fu D, et al. Photoelectrochemical TiO₂-Au-nanowire-based motor for precise modulation of single-neuron activities. *Adv Funct Mater*. 2021; 31: 2008667.
- Li Z, Xu J, Wu Z, Guo B, He Q. Liquid metal swimming nanorobots. *Acc Mater Res*. 2022; 3: 122-32.
- Liu L, Chen B, Liu K, Gao J, Ye Y, Wang Z, et al. Wireless manipulation of magnetic/piezoelectric micromotors for precise neural stem-like cell stimulation. *Adv Funct Mater*. 2020; 30: 1910108.
- Xu H, Medina-Sanchez M, Schmidt OG. Magnetic micromotors for multiple motile sperm cells capture, transport, and enzymatic release. *Angew Chem Int Ed Engl*. 2020; 59: 15029-37.
- He X, Jiang H, Li J, Ma Y, Fu B, Hu C. Dipole-moment induced phototaxis and fuel-free propulsion of ZnO/Pt Janus micromotors. *Small*. 2021; 17: 2101388.
- Kim JT, Choudhury U, Jeong HH, Fischer P. Nanodiamonds that swim. *Adv Mater*. 2017; 29: 1701024.
- Xie L, Liu T, He Y, Zeng J, Zhang W, Liang Q, et al. Kinetics-regulated interfacial selective superassembly of asymmetric smart nanovehicles with tailored topological hollow architectures. *Angew Chem Int Ed Engl*. 2022; 61: e202200240.
- Xu F, Crespi S, Pacella G, Fu YX, Stuart MCA, Zhang Q, et al. Dynamic control of a multistate chiral supramolecular polymer in water. *J Am Chem Soc*. 2022; 144: 6019-27.
- Sun M, Liu Q, Fan X, Wang Y, Chen W, Tian C, et al. Autonomous biohybrid urchin-like microporator for intracellular payload delivery. *Small*. 2020; 16: 1906701.
- Wang X, Chen XZ, Alcantara CCJ, Sevim S, Hoop M, Terzopoulou A, et al. MOFBOTS: Metal-organic-framework-based biomedical microrobots. *Adv Mater*. 2019; 31: 1901592.
- Wang Y, Liu Y, Li Y, Xu D, Pan X, Chen Y, et al. Magnetic nanomotor-based maneuverable SERS probe. *Research*. 2020; 2020: 7962024.
- Lu X, Wei Y, Ou H, Zhao C, Shi L, Liu W. Universal control for micromotor swarms with a hybrid sonoelectrode. *Small*. 2021; 17: 2104516.
- Ren L, Wang W, Mallouk TE. Two forces are better than one: Combining chemical and acoustic propulsion for enhanced micromotor functionality. *Acc Chem Res*. 2018; 51: 1948-56.
- Wang Z, Xu W, Wang Z, Lyu D, Mu Y, Duan W, et al. Polyhedral micromotors of metal-organic frameworks: Symmetry breaking and propulsion. *J Am Chem Soc*. 2021; 143: 19881-92.
- Ying Y, Plutnar J, Pumeras M. Six-degree-of-freedom steerable visible-light-driven microsubmarines using water as a fuel: Application for explosives decontamination. *Small*. 2021; 17: 2100294.
- Llopis-Lorente A, Garcia-Fernandez A, Murillo-Cremaes N, Hortelao AC, Patino T, Villalonga R, et al. Enzyme-powered gated mesoporous silica nanomotors for on-command intracellular payload delivery. *ACS Nano*. 2019; 13: 12171-83.

36. Wang Q, Dong R, Wang C, Xu S, Chen D, Liang Y, et al. Glucose-fueled micromotors with highly efficient visible-light photocatalytic propulsion. *ACS Appl Mater Interfaces*. 2019; 11: 6201-7.
37. Gao S, Hou J, Zeng J, Richardson JJ, Gu Z, Gao X, et al. Superassembled biocatalytic porous framework micromotors with reversible and sensitive pH-speed regulation at ultralow physiological H₂O₂ concentration. *Adv Funct Mater*. 2019; 29: 1808900.
38. Yuan K, Jurado-Sanchez B, Escarpa A. Dual-propelled lanibiotic based Janus micromotors for selective inactivation of bacterial biofilms. *Angew Chem Int Ed Engl*. 2021; 60: 4915-24.
39. de Avila BE, Angsantikul P, Li J, Angel Lopez-Ramirez M, Ramirez-Herrera DE, Thamphiwatana S, et al. Micromotor-enabled active drug delivery for *in vivo* treatment of stomach infection. *Nat Commun*. 2017; 8: 272.
40. Karshalev E, Esteban-Fernandez de Avila B, Beltran-Gastelum M, Angsantikul P, Tang S, Mundaca-Urbe R, et al. Micromotor pills as a dynamic oral delivery platform. *ACS Nano*. 2018; 12: 8397-405.
41. Nourhani A, Karshalev E, Soto F, Wang J. Multigear bubble propulsion of transient micromotors. *Research*. 2020; 2020: 7823615.
42. Xu X, Huo Z, Guo J, Liu H, Qi X, Wu Z. Micromotor-derived composites for biomedicine delivery and other related purposes. *Biodes Manuf*. 2020; 3: 133-47.
43. Li J, Liu W, Wang J, Rozen I, He S, Chen C, et al. Nanoconfined atomic layer deposition of TiO₂/Pt nanotubes: Toward ultrasmall highly efficient catalytic nanorockets. *Adv Funct Mater*. 2017; 27: 1700598.
44. Zhang X, Xie W, Wang H, Zhang Z. Magnetic matchstick micromotors with switchable motion modes. *Chem Commun*. 2021; 57: 3797-800.
45. Pumm AK, Engelen W, Kopperger E, Isensee J, Vogt M, Kozina V, et al. A DNA origami rotary ratchet motor. *Nature*. 2022; 607: 492-8.
46. Hwang J, Yang HM, Lee KW, Jung YI, Lee KJ, Park CW. A remotely steerable Janus micromotor adsorbent for the active remediation of Cs-contaminated water. *J Hazard Mater*. 2019; 369: 416-22.
47. Lin X, Xu B, Zhao Z, Yang X, Xing Y, You C, et al. Flying squirrel-inspired motion control of a light-deformed Pt-PAzoMA micromotor through drag force manipulation. *ACS Appl Mater Interfaces*. 2021; 13: 30106-17.
48. Park CW, Kim T, Yang HM, Lee Y, Kim HJ. Active and selective removal of Cs from contaminated water by self-propelled magnetic illite microspheres. *J Hazard Mater*. 2021; 416: 126226.
49. Lee Y, Park CW, Kim HJ, Kim SJ, Lee TS, Yang HM. Sulfur-encapsulated zeolite micromotors for the selective removal of cesium from high-salt water with accelerated cleanup times. *Chemosphere*. 2021; 276: 130190.
50. Wan M, Wang Q, Wang R, Wu R, Li T, Fang D, et al. Platelet-derived porous nanomotor for thrombus therapy. *Sci Adv*. 2020; 6: eaaz9014.
51. Xuan M, Wu Z, Shao J, Dai L, Si T, He Q. Near infrared light-powered Janus mesoporous silica nanoparticle motors. *J Am Chem Soc*. 2016; 138: 6492-7.
52. Zhang F, Mundaca-Urbe R, Gong H, Esteban-Fernandez de Avila B, Beltran-Gastelum M, Karshalev E, et al. A macrophage-magnesium hybrid biomotor: Fabrication and characterization. *Adv Mater*. 2019; 31: 1901828.
53. Wang Z, Wang S, Liu K, Fu D, Ye Y, Gao J, et al. Water powered and anti-CD3 loaded mg micromotor for t cell activation. *Appl Mater Today*. 2020; 21: 100839.
54. Liu K, Ou J, Wang S, Gao J, Liu L, Ye Y, et al. Magnesium-based micromotors for enhanced active and synergistic hydrogen chemotherapy. *Appl Mater Today*. 2020; 20: 100694.
55. Zhou M, Hou T, Li J, Yu S, Xu Z, Yin M, et al. Self-propelled and targeted drug delivery of poly(aspartic acid)/iron-Zinc microrocket in the stomach. *ACS Nano*. 2019; 13: 1324-32.
56. Karshalev E, Chen C, Marolt G, Martin A, Campos I, Castillo R, et al. Utilizing iron's attractive chemical and magnetic properties in microrocket design, extended motion, and unique performance. *Small*. 2017; 13: 1700035.
57. Esteban-Fernandez de Avila B, Lopez-Ramirez MA, Mundaca-Urbe R, Wei X, Ramirez-Herrera DE, Karshalev E, et al. Multicompartment tubular micromotors toward enhanced localized active delivery. *Adv Mater*. 2020; 32: 2000091.
58. Cui Q, Le T-H, Lin Y-J, Miao Y-B, Sung IT, Tsai W-B, et al. A self-powered battery-driven drug delivery device that can function as a micromotor and galvanically actuate localized payload release. *Nano Energy*. 2019; 66: 104120.
59. Lin Z, Gao C, Wang D, He Q. Bubble-propelled Janus gallium/zinc micromotors for the active treatment of bacterial infections. *Angew Chem Int Ed Engl*. 2021; 60: 8750-4.
60. Xuan M, Shao J, Gao C, Wang W, Dai L, He Q. Self-propelled nanomotors for thermomechanically percolating cell membranes. *Angew Chem Int Ed Engl*. 2018; 57: 12463-7.
61. Shao J, Abdelghani M, Shen G, Cao S, Williams DS, van Hest JCM. Erythrocyte membrane modified Janus polymeric motors for thrombus therapy. *ACS Nano*. 2018; 12: 4877-85.
62. Zheng S, Wang Y, Pan S, Ma E, Jin S, Jiao M, et al. Biocompatible nanomotors as active diagnostic imaging agents for enhanced magnetic resonance imaging of tumor tissues *in vivo*. *Adv Funct Mater*. 2021; 31: 2100936.
63. Lin F, Shao Y, Wu Y, Zhang Y. NIR light-propelled Janus-based nanoplatform for cytosolic-fueled microRNA imaging. *ACS Appl Mater Interfaces*. 2021; 13: 3713-21.
64. Chen L, Yuan H, Chen S, Zheng C, Wu X, Li Z, et al. Cost-effective, high-yield production of biotemplated catalytic tubular micromotors as self-propelled microcleaners for water treatment. *ACS Appl Mater Interfaces*. 2021; 13: 31226-35.
65. Yang J, Li J, Ng DHL, Yang P, Yang W, Liu Y. Micromotor-assisted highly efficient Fenton catalysis by a laccase/Fe-BTC-NiFe₂O₄ nanozyme hybrid with a 3D hierarchical structure. *Environ Sci Nano*. 2020; 7: 2573-83.
66. Xie H, Sun M, Fan X, Lin Z, Chen W, Wang L, et al. Reconfigurable magnetic microrobot swarm: Multimode transformation, locomotion, and manipulation. *Sci Robot*. 2019; 4: eaav8006.
67. Rutkowski S, Si T, Gai M, Sun M, Frueh J, He Q. Magnetically-guided hydrogel capsule motors produced via ultrasound assisted hydrodynamic electro-spray ionization jetting. *J Colloid Interface Sci*. 2019; 541: 407-17.
68. Wang Z, Fu D, Xie D, Fu S, Wu J, Wang S, et al. Magnetic helical hydrogel motor for directing T cell chemotaxis. *Adv Funct Mater*. 2021; 31: 2101648.
69. Li Q, Chen H, Feng X, Yu C, Feng F, Chai Y, et al. Nanoparticle-regulated semiautonomous magnetotactic bacteria with tunable magnetic moment and magnetic sensitivity. *Small*. 2019; 15: 1900427.
70. Wu J, Ma S, Li M, Hu X, Jiao N, Tung S, et al. Enzymatic/magnetic hybrid micromotors for synergistic anticancer therapy. *ACS Appl Mater Interfaces*. 2021; 13: 31514-26.
71. Yang Q, Xu H, Wen H, Zhao H, Liu X, Cai Y, et al. Graphene oxide induced enhancement of light-driven micromotor with biocompatible fuels. *Appl Mater Today*. 2021; 22: 100943.
72. Kwon T, Kumari N, Kumar A, Lim J, Son CY, Lee IS. Au/Pt-egg-in-nest nanomotor for glucose-powered catalytic motion and enhanced molecular transport to living cells. *Angew Chem Int Ed Engl*. 2021; 60: 17579-86.
73. Yuan Y, Gao C, Wang Z, Fan J, Zhou H, Wang D, et al. Upconversion-nanoparticle-functionalized Janus micromotors for efficient detection of uric acid. *J Mater Chem B*. 2022; 10: 358-63.
74. Kadiri VM, Bussi C, Holle AW, Son K, Kwon H, Schutz G, et al. Biocompatible magnetic micro- and nanodevices: Fabrication of FePt nanopropellers and cell transfection. *Adv Mater*. 2020; 32: 2001114.
75. Xiao Z, Duan S, Xu P, Cui J, Zhang H, Wang W. Synergistic speed enhancement of an electric-photochemical hybrid micromotor by tilt rectification. *ACS Nano*. 2020; 14: 8658-67.
76. Panda A, Reddy AS, Venkateswarlu S, Yoon M. Bio-inspired self-propelled diatom micromotor by catalytic decomposition of H₂O₂ under low fuel concentration. *Nanoscale*. 2018; 10: 16268-77.
77. Chen C, Karshalev E, Guan J, Wang J. Magnesium-based micromotors: Water-powered propulsion, multifunctionality, and biomedical and environmental applications. *Small*. 2018; 14: 1704252.
78. Rosli NF, Mayorga-Martinez CC, Fisher AC, Alduhaish O, Webster RD, Pumera M. Arsenene nanomotors as anticancer drug carrier. *Appl Mater Today*. 2020; 21: 100819.
79. Xiong K, Xu L, Lin J, Mou F, Guan J. Mg-based micromotors with motion responsive to dual stimuli. *Research*. 2020; 2020: 6213981.
80. Wang H, Liang Y, Gao W, Dong R, Wang C. Emulsion hydrogel soft motor actuated by thermal stimulation. *ACS Appl Mater Interfaces*. 2017; 9: 43211-9.
81. Zhou X, Li Z, Tan L, Zhang Y, Jiao Y. Near-infrared light-steered graphene aerogel micromotor with high speed and precise navigation for active transport and microassembly. *ACS Appl Mater Interfaces*. 2020; 12: 23134-44.
82. Barrio J, Volokh M, Shalom M. Polymeric carbon nitrides and related metal-free materials for energy and environmental applications. *J Mater Chem A Mater*. 2020; 8: 11075-116.
83. Dong T, Sun M, Hu K, Wang Q, Lu C, Kou J. Self-propelled jet carbon micromotor enhanced photocatalytic performance for water splitting. *Int J Hydrogen Energy*. 2021; 46: 17187-96.
84. Zheng J, Dai B, Wang J, Xiong Z, Yang Y, Liu J, et al. Orthogonal navigation of multiple visible-light-driven artificial microswimmers. *Nat Commun*. 2017; 8: 1438.
85. Wan M, Chen H, Wang Q, Niu Q, Xu P, Yu Y, et al. Bio-inspired nitric-oxide-driven nanomotor. *Nat Commun*. 2019; 10: 966.
86. Ye J, Fu Q, Liu L, Chen L, Zhang X, Li Q, et al. Ultrasound-propelled Janus Au NR-mSiO₂ nanomotor for NIR-II photoacoustic imaging guided sonodynamic-gas therapy of large tumors. *Sci China Chem*. 2021; 64: 2218-29.
87. Fan W, Yung BC, Chen X. Stimuli-responsive NO release for on-demand gas-sensitized synergistic cancer therapy. *Angew Chem Int Ed Engl*. 2018; 57: 8383-94.
88. Deng Q, Zhang L, Lv W, Liu X, Ren J, Qu X. Biological mediator-propelled nanosweeper for nonpharmaceutical thrombus therapy. *ACS Nano*. 2021; 15: 6604-13.
89. Kang C, Gwon S, Song C, Kang PM, Park SC, Jeon J, et al. Fibrin-targeted and H₂O₂-responsive nanoparticles as a theranostics for thrombosed vessels. *ACS Nano*. 2017; 11: 6194-203.
90. Tong J, Wang D, Liu Y, Lou X, Jiang J, Dong B, et al. Bioinspired micro/nanomotor with visible light energy-dependent forward, reverse, reciprocating, and spinning schooling motion. *Proc Natl Acad Sci U S A*. 2021; 118: e2104481118.
91. Zhu L, Ding T, Gao M, Peh KKN, Ho GW. Shape conformal and thermal insulative organic solar absorber sponge for photothermal water evaporation and thermoelectric power generation. *Adv Energy Mater*. 2019; 9: 1900250.
92. Yang W, Li J, Xu Z, Yang J, Liu Y, Liu L. A Eu-MOF/EDTA-NiAl-CLDH fluorescent micromotor for sensing and removal of Fe³⁺ from water. *J Mater Chem C Mater*. 2019; 7: 10297-308.
93. Mujtaba J, Liu J, Dey KK, Li T, Chakraborty R, Xu K, et al. Micro-bio-chemo-mechanical-systems: Micromotors, microfluidics, and nanozymes for biomedical applications. *Adv Mater*. 2021; 33: 2007465.

94. Liu M, Chen L, Zhao Z, Liu M, Zhao T, Ma Y, et al. Enzyme-based mesoporous nanomotors with near-infrared optical brakes. *J Am Chem Soc.* 2022; 144: 3892-901.
95. Wang L, Marciello M, Estevez-Gay M, Soto Rodriguez PED, Luengo Morato Y, Iglesias-Fernandez J, et al. Enzyme conformation influences the performance of lipase-powered nanomotors. *Angew Chem Int Ed Engl.* 2020; 59: 21080-7.
96. Yuan H, Liu X, Wang L, Ma X. Fundamentals and applications of enzyme powered micro/nano-motors. *Bioact Mater.* 2021; 6: 1727-49.
97. Feng M, Gilson MK. Enhanced diffusion and chemotaxis of enzymes. *Annu Rev Biophys.* 2020; 49: 87-105.
98. Hortelão AC, Patiño T, Perez-Jiménez A, Blanco À, Sánchez S. Enzyme-powered nanobots enhance anticancer drug delivery. *Adv Funct Mater.* 2018; 28: 1705086.
99. Zhang Z, Yan H, Li S, Liu Y, Ran P, Chen W, et al. Janus rod-like micromotors to promote the tumor accumulation and cell internalization of therapeutic agents. *Chem Eng J.* 2021; 404: 127073.
100. Tang S, Zhang F, Gong H, Wei F, Zhuang J, Karshalev E, et al. Enzyme-powered Janus platelet cell robots for active and targeted drug delivery. *Sci Robot.* 2020; 5: eaba6137.
101. Jiao C, Zhao C, Ma Y, Yang W. A versatile strategy to coat individual cell with fully/partially covered shell for preparation of self-propelling living cells. *ACS Nano.* 2021; 15: 15920-9.
102. Fu S, Zhang X, Xie Y, Wu J, Ju H. An efficient enzyme-powered micromotor device fabricated by cyclic alternate hybridization assembly for DNA detection. *Nanoscale.* 2017; 9: 9026-33.
103. Wang J, Toebes BJ, Plachokova AS, Liu Q, Deng D, Jansen JA, et al. Self-propelled PLGA micromotor with chemotactic response to inflammation. *Adv Healthc Mater.* 2020; 9: 1901710.
104. Zhao L, Liu Y, Xie S, Ran P, Wei J, Liu Q, et al. Janus micromotors for motion-capture-ratiometric fluorescence detection of circulating tumor cells. *Chem Eng J.* 2020; 382: 123041.
105. Zhao L, Xie S, Liu Y, Liu Q, Song X, Li X. Janus micromotors for motion-capture-lighting of bacteria. *Nanoscale.* 2019; 11: 17831-40.
106. Sun J, Mathesh M, Li W, Wilson DA. Enzyme-powered nanomotors with controlled size for biomedical applications. *ACS Nano.* 2019; 13: 10191-200.
107. Yang Y, Arque X, Patino T, Guillerm V, Blerch PR, Perez-Carvajal J, et al. Enzyme-powered porous micromotors built from a hierarchical micro- and mesoporous UiO-type metal-organic framework. *J Am Chem Soc.* 2020; 142: 20962-7.
108. Dey KK, Zhao X, Tansi BM, Mendez-Ortiz WJ, Cordova-Figueroa UM, Golestanian R, et al. Micromotors powered by enzyme Catalysis. *Nano Lett.* 2015; 15: 8311-5.
109. Gao C, Zhou C, Lin Z, Yang M, He Q. Surface wettability-directed propulsion of glucose-powered nanoflask motors. *ACS Nano.* 2019; 13: 12758-66.
110. You Y, Xu D, Pan X, Ma X. Self-propelled enzymatic nanomotors for enhancing synergetic photodynamic and starvation therapy by self-accelerated cascade reactions. *Appl Mater Today.* 2019; 16: 508-17.
111. Wu J, Wang X, Wang Q, Lou Z, Li S, Zhu Y, et al. Nanomaterials with enzyme-like characteristics (nanozymes): next-generation artificial enzymes (II). *Chem Soc Rev.* 2019; 48: 1004-76.
112. Scott S, Zhao H, Dey A, Gunnoe TB. Nano-apples and orange-zymes. *ACS Catal.* 2020; 10: 14315-7.
113. Chen WJ, Zhou H, Zhang B, Cao QH, Wang B, Ma X. Recent progress of micro/nanorobots for cell delivery and manipulation. *Adv Funct Mater.* 2022; 32: 2110625.
114. Peng F, Tu Y, Wilson DA. Micro/nanomotors towards *in vivo* application: cell, tissue and biofluid. *Chem Soc Rev.* 2017; 46: 5289-310.
115. Guo Y, Cao X, Zhang S. Au-Fe₃O₄ nanoagent coated cell membrane for targeted delivery and enhanced chem/photo therapy. *Chem Commun.* 2021; 57: 10504-7.
116. Guo Y, Zheng X, Gai T, Wei Z, Zhang S. Co-biomembrane-coated Fe₃O₄/MnO₂ multifunctional nanoparticles for targeted delivery and enhanced chemodynamic/photothermal/chemo therapy. *Chem Commun.* 2021; 57: 5754-7.
117. Magdanz V, Medina-Sanchez M, Schwarz L, Xu H, Elgeti J, Schmidt OG. Spermatozoa as functional components of robotic microswimmers. *Adv Mater.* 2017; 29: 1606301.
118. Magdanz V, Sanchez S, Schmidt OG. Development of a sperm-flagella driven micro-bio-robot. *Adv Mater.* 2013; 25: 6581-8.
119. Gaffney EA, Ishimoto K, Walker BJ. Modelling motility: The mathematics of spermatozoa. *Front Cell Dev Biol.* 2021; 9: 710825.
120. Chen C, Chang X, Angsantikul P, Li J, Esteban-Fernández de Ávila B, Karshalev E, et al. Chemotactic guidance of synthetic organic/inorganic payloads functionalized sperm micromotors. *Adv Biosys.* 2017; 2: 1700160.
121. Xu H, Medina-Sanchez M, Magdanz V, Schwarz L, Hebenstreit F, Schmidt OG. Sperm-hybrid micromotor for targeted drug delivery. *ACS Nano.* 2018; 12: 327-37.
122. Ishimoto K, Gaffney EA. Mechanical tuning of mammalian sperm behaviour by hyperactivation, rheology and substrate adhesion: a numerical exploration. *J R Soc Interface.* 2016; 13: 20160633.
123. Xu H, Medina-Sanchez M, Maitz MF, Werner C, Schmidt OG. Sperm micromotors for cargo delivery through flowing blood. *ACS Nano.* 2020; 14: 2982-93.
124. Wadhwa N, Tu Y, Berg HC. Mechanosensitive remodeling of the bacterial flagellar motor is independent of direction of rotation. *Proc Natl Acad Sci U S A.* 2021; 118: e2024608118.
125. Park BW, Zhuang J, Yasa O, Sitti M. Multifunctional bacteria-driven microswimmers for targeted active drug delivery. *ACS Nano.* 2017; 11: 8910-23.
126. Zai W, Kang L, Dong T, Wang H, Yin L, Gan S, et al. E. coli membrane vesicles as a catalase carrier for long-term tumor hypoxia relief to enhance radiotherapy. *ACS Nano.* 2021; 15: 15381-94.
127. Zhuang J, Sitti M. Chemotaxis of bio-hybrid multiple bacteria-driven microswimmers. *Sci Rep.* 2016; 6: 32135.
128. Alapan Y, Yasa O, Schauer O, Giltinan J, Tabak AF, Sourjik V, et al. Soft erythrocyte-based bacterial microswimmers for cargo delivery. *Sci Robot.* 2018; 3: eaar4423.
129. Stanton MM, Park BW, Vilela D, Bente K, Faivre D, Sitti M, et al. Magnetotactic bacteria powered biohybrids target E. coli biofilms. *ACS Nano.* 2017; 11: 9968-78.
130. Vincenti B, Ramos G, Cordero ML, Douarche C, Soto R, Clement E. Magnetotactic bacteria in a droplet self-assemble into a rotary motor. *Nat Commun.* 2019; 10: 5082.
131. Ribeiro AJS, Guth BD, Engwall M, Eldridge S, Foley CM, Guo L, et al. Considerations for an *in vitro*, cell-based testing platform for detection of drug-induced inotropic effects in early drug development. Part 2: Designing and fabricating microsystems for assaying cardiac contractility with physiological relevance using human iPSC-cardiomyocytes. *Front Pharmacol.* 2019; 10: 934.
132. Wu S, Duan B, Qin X, Butcher JT. Nanofiber-structured hydrogel yarns with pH-response capacity and cardiomyocyte-drivability for bio-microactuator application. *Acta Biomater.* 2017; 60: 144-53.
133. Shang Y, Chen Z, Fu F, Sun L, Shao C, Jin W, et al. Cardiomyocyte-driven structural color actuation in anisotropic inverse opals. *ACS Nano.* 2019; 13: 796-802.
134. Fu F, Shang L, Chen Z, Yu Y, Zhao Y. Bioinspired living structural color hydrogels. *Sci Robot.* 2018; 3: eaar8580.
135. Sun L, Chen Z, Bian F, Zhao Y. Bioinspired soft robotic caterpillar with cardiomyocyte drivers. *Adv Funct Mater.* 2019; 30: 1907820.
136. Xu B, Han X, Hu Y, Luo Y, Chen CH, Chen Z, et al. A remotely controlled transformable soft robot based on engineered cardiac tissue construct. *Small.* 2019; 15: 1900006.
137. Akiyama Y, Odaira K, Sakiyama K, Hoshino T, Iwabuchi K, Morishima K. Rapidly-moving insect muscle-powered microrobot and its chemical acceleration. *Biomed Microdevices.* 2012; 14: 979-86.
138. Akiyama Y, Hoshino T, Iwabuchi K, Morishima K. Room temperature operable autonomously moving bio-microrobot powered by insect dorsal vessel tissue. *PLoS One.* 2012; 7: e38274.
139. Uesugi K, Shimizu K, Akiyama Y, Hoshino T, Iwabuchi K, Morishima K. Contractile performance and controllability of insect muscle-powered bioactuator with different stimulation strategies for soft robotics. *Soft Robot.* 2016; 3: 13-22.
140. Cvetkovic C, Raman R, Chan V, Williams BJ, Tolish M, Bajaj P, et al. Three-dimensionally printed biological machines powered by skeletal muscle. *Proc Natl Acad Sci U S A.* 2014; 111: 10125-30.
141. Raman R, Grant L, Seo Y, Cvetkovic C, Gapsinske M, Palasz A, et al. Damage, healing, and remodeling in optogenetic skeletal muscle bioactuators. *Adv Healthc Mater.* 2017; 6: 1700030.
142. Li Z, Seo Y, Aydin O, Elhebeary M, Kamm RD, Kong H, et al. Biohybrid valveless pump-bot powered by engineered skeletal muscle. *Proc Natl Acad Sci U S A.* 2019; 116: 1543-8.
143. Hasebe A, Suematsu Y, Takeoka S, Mazzocchi T, Vannozzi L, Ricotti L, et al. Biohybrid actuators based on skeletal muscle-powered microgrooved ultrathin films consisting of poly(styrene-block-butadiene-block-styrene). *ACS Biomater Sci Eng.* 2019; 5: 5734-43.
144. Aydin O, Zhang X, Nuethong S, Pagan-Diaz GJ, Bashir R, Gazzola M, et al. Neuromuscular actuation of biohybrid motile bots. *Proc Natl Acad Sci U S A.* 2019; 116: 19841-7.
145. Liu L, Wu J, Chen B, Gao J, Li T, Ye Y, et al. Magnetically actuated biohybrid microswimmers for precise photothermal muscle contraction. *ACS Nano.* 2022; 16: 6515-26.
146. Akolpoglu MB, Alapan Y, Dogan NO, Baltaci SF, Yasa O, Aybar Tural G, et al. Magnetically steerable bacterial microrobots moving in 3D biological matrices for stimuli-responsive cargo delivery. *Sci Adv.* 2022; 8: eabo6163.
147. Dong Y, Yi C, Yang S, Wang J, Chen P, Liu X, et al. A substrate-free graphene oxide-based micromotor for rapid adsorption of antibiotics. *Nanoscale.* 2019; 11: 4562-70.
148. Cai L, Wang H, Yu Y, Bian F, Wang Y, Shi K, et al. Stomatocyte structural color-barcode micromotors for multiplex assays. *Natl Sci Rev.* 2020; 7: 644-51.
149. Bandari VK, Nan Y, Karnaushenko D, Hong Y, Sun B, Striggow F, et al. A flexible microsystem capable of controlled motion and actuation by wireless power transfer. *Nat Electron.* 2020; 3: 172-80.
150. Guo Z, Wang T, Rawal A, Hou J, Cao Z, Zhang H, et al. Biocatalytic self-propelled submarine-like metal-organic framework microparticles with pH-triggered buoyancy control for directional vertical motion. *Mater Today.* 2019; 28: 10-6.

151. Gao C, Lin Z, Wang D, Wu Z, Xie H, He Q. Red blood cell-mimicking micromotor for active photodynamic cancer therapy. *ACS Appl Mater Interfaces*. 2019; 11: 23392-400.
152. Guo Y, Liu F, Hu Y, Zheng X, Cao X, Zhu Y, et al. Activated plasmonic nanoaggregates for dark-field *in situ* imaging for HER2 protein Imaging on cell surfaces. *Bioconjug Chem*. 2020; 31: 631-8.
153. Guo Y, Cao X, Zheng X, Abbas SKJ, Li J, Tan W. Construction of nanocarriers based on nucleic acids and their applications in nanobiology delivery systems. *Natl Sci Rev*. 2022; 9: nwac006.
154. Jiang Q, Liu L, Li Q, Cao Y, Chen D, Du Q, et al. NIR-laser-triggered gadolinium-doped carbon dots for magnetic resonance imaging, drug delivery and combined photothermal chemotherapy for triple negative breast cancer. *J Nanobiotechnology*. 2021; 19: 64.
155. Wang Q, Wang Y, Guo B, Shao S, Yu Y, Zhu X, et al. Novel heparin-loaded mesoporous tubular micromotors formed via template-assisted electrochemical deposition. *J Mater Chem B*. 2019; 7: 2688-95.
156. Hils C, Schmelz J, Drechsler M, Schmalz H. Janus micelles by crystallization-driven self-assembly of an amphiphilic, double-crystalline triblock terpolymer. *J Am Chem Soc*. 2021; 143: 15582-6.
157. Gao C, Wang Y, Ye Z, Lin Z, Ma X, He Q. Biomedical micro-/nanomotors: From overcoming biological barriers to *in vivo* imaging. *Adv Mater*. 2021; 33: 2000512.
158. Zhang X, Chen C, Wu J, Ju H. Bubble-propelled jellyfish-like micromotors for DNA Sensing. *ACS Appl Mater Interfaces*. 2019; 11: 13581-8.
159. Zhang Y, Yang F, Wei W, Wang Y, Yang S, Li J, et al. Self-propelled Janus mesoporous micromotor for enhanced microRNA capture and amplified detection in complex biological samples. *ACS Nano*. 2022; 16: 5587-96.
160. Cogal GC, Karaca GY, Uygun E, Kuralay F, Oksuz L, Remskar M, et al. RF plasma-enhanced conducting Polymer/W₃O₄ based self-propelled micromotors for miRNA detection. *Anal Chim Acta*. 2020; 1138: 69-78.
161. Molinero-Fernandez A, Moreno-Guzman M, Arruza L, Lopez MA, Escarpa A. Polymer-based micromotor fluorescence immunoassay for on-the-move sensitive procalcitonin determination in very low birth weight infants' plasma. *ACS Sens*. 2020; 5: 1336-44.
162. de Avila BE, Zhao M, Campuzano S, Ricci F, Pingarron JM, Mascini M, et al. Rapid micromotor-based naked-eye immunoassay. *Talanta*. 2017; 167: 651-7.
163. Guo J, Li Y, Wang B, Chen W, Chen S, Liu S, et al. Self-propelled Janus nanomotor as active probe for detection of pepsinogen by lateral flow immunoassay. *Mikrochim Acta*. 2022; 189: 468.
164. Qi S, Sun YH, Dong XZ, Khan IM, Lv Y, Zhang Y, et al. Bispecific aptamer-initiated 3D DNA nanomotor biosensor powered by DNAzyme and entropy-driven circuit for sensitive and specificity detection of lysozyme. *Nano Res*. 2023; 16: 1286-1295.
165. Ma E, Wang K, Wang H. An immunoassay based on nanomotor-assisted electrochemical response for the detection of immunoglobulin. *Mikrochim Acta*. 2022; 189: 47.
166. Hu Y, Li Z, Sun Y. Ultrasmall enzyme/light-powered nanomotor facilitates cholesterol detection. *J Colloid Interface Sci*. 2022; 621: 341-51.
167. Liu X, Chen W, Zhao D, Liu X, Wang Y, Chen Y, et al. Enzyme-powered hollow nanorobots for active microsampling enabled by thermoresponsive polymer gating. *ACS Nano*. 2022; 16: 10354-63.
168. Wan Y, Fu L, Li C, Lin J, Huang P. Conquering the hypoxia limitation for photodynamic therapy. *Adv Mater*. 2021; 33: 2103978.
169. Chen DY, Jin ZK, Zhao B, Wang YS, He QJ. MBene as a theranostic nanoplatform for photocontrolled intratumoral retention and drug release. *Adv Mater*. 2021; 33: 2008089.
170. Zhou JR, Karshalev E, Mundaca-Urbe R, de Avila BEF, Krishnan N, Xiao C, et al. Physical disruption of solid tumors by immunostimulatory microrobots enhances antitumor immunity. *Adv Mater*. 2021; 33: 2103505.
171. Xing Y, Zhou M, Liu X, Qiao M, Zhou L, Xu T, et al. Bioinspired jellyfish-like carbon/manganese nanomotors with H₂O₂ and NIR light dual-propulsion for enhanced tumor penetration and chemodynamic therapy. *Chem Eng J*. 2023; 461: 142142.
172. Cai L, Zhao C, Chen H, Fan L, Zhao Y, Qian X, et al. Suction-cup-inspired adhesive micromotors for drug delivery. *Adv Sci*. 2022; 9: 2103384.
173. Li X, Wu R, Chen H, Li T, Jiang H, Xu X, et al. Near-infrared light-driven multifunctional tubular micromotors for treatment of atherosclerosis. *ACS Appl Mater Interfaces*. 2021; 13: 30930-40.
174. Schwarz L, Karnaushenko DD, Hebenstreit F, Naumann R, Schmidt OG, Medina-Sanchez M. A rotating spiral micromotor for noninvasive zygote transfer. *Adv Sci*. 2020; 7: 2000843.
175. Ji X, Yang H, Liu W, Ma Y, Wu J, Zong X, et al. Multifunctional parachute-like nanomotors for enhanced skin penetration and synergistic antifungal therapy. *ACS Nano*. 2021; 15: 14218-28.
176. Cong Z, Tang S, Xie L, Yang M, Li Y, Lu D, et al. Magnetic-powered Janus cell robots loaded with oncolytic adenovirus for active and targeted virotherapy of bladder cancer. *Adv Mater*. 2022; 34: 2201042.
177. Li Y, Wu J, Oku H, Ma G. Polymer-modified micromotors with biomedical applications: Promotion of functionalization. *Adv Nanobiomed Res*. 2022; 2: 2200074.
178. Guo Y, Li W, Liu S, Jing D, Wang Y, Feng Q, et al. Construction of nanocarriers based on endogenous cell membrane and their application in nanomedicine. *Chin J Chem*. 2022; 40: 1623-40.
179. Yu Y, Guo J, Wang Y, Shao C, Wang Y, Zhao Y. Bioinspired helical micromotors as dynamic cell microcarriers. *ACS Appl Mater Interfaces*. 2020; 12: 16097-103.
180. Lv J, Xing Y, Xu T, Zhang X, Du X. Advanced micro/nanomotors for enhanced bioadhesion and tissue penetration. *Appl Mater Today*. 2021; 23: 101034.
181. Guo Y, Wu D, Zhang X, Zhang K, Luo Y. Biomolecules in cell-derived extracellular vesicle chariots as warriors to repair damaged tissues. *Nanoscale*. 2021; 13: 16017-33.
182. Wang L, Guo P, Jin D, Peng Y, Sun X, Chen Y, et al. Enzyme-powered tubular microrobotic jets as bioinspired micropumps for active transmembrane drug transport. *ACS Nano*. 2023; 17: 5095-107.
183. Choi H, Jeong SH, Kim TY, Yi J, Hahn SK. Bioinspired urease-powered micromotor as an active oral drug delivery carrier in stomach. *Bioact Mater*. 2022; 9: 54-62.
184. Chen H, Shi T, Wang Y, Liu Z, Liu F, Zhang H, et al. Deep penetration of nanolevel drugs and micrometer-level T cells promoted by nanomotors for cancer immunochemotherapy. *J Am Chem Soc*. 2021; 143: 12025-37.
185. Park Y, Yoon HJ, Lee SE, Lee LP. Multifunctional cellular Targeting, molecular delivery, and imaging by integrated mesoporous-silica with optical nanocrescent antenna: MONA. *ACS Nano*. 2022; 16: 2013-23.
186. Li Q, Liu L, Huo H, Su L, Wu Y, Lin H, et al. Nanosized Janus AuNR-Pt motor for enhancing NIR-II photoacoustic imaging of deep tumor and Pt²⁺ ion-based chemotherapy. *ACS Nano*. 2022; 16: 7947-60.
187. Vilela D, Blanco-Cabra N, Eguskiza A, Hortelao AC, Torrents E, Sanchez S. Drug-free enzyme-based bactericidal nanomotors against pathogenic bacteria. *ACS Appl Mater Interfaces*. 2021; 13: 14964-73.
188. Wu Z, Zhou M, Tang X, Zeng J, Li Y, Sun Y, et al. Carrier-free trehalose-based nanomotors targeting macrophages in inflammatory plaque for treatment of atherosclerosis. *ACS Nano*. 2022; 16: 3808-20.
189. Guo Y, Sun L, Wang Y, Wang Q, Jing D, Liu S. Nanomaterials based on thermosensitive polymer in biomedical field. *Front Chem*. 2022; 10: 946183.

Author biographies



Yingshu Guo was born in 1986 and received her PhD from Qingdao University of Science and Technology in 2012. Currently, she is the Professor in Qilu University of Technology and she research involves biosensing and biomaterial. She has published 45 scientific articles.



Dan Jing was born in 1992 and received her B.S. degree from Shanxi Datong University in 2015. She is now studying for a Master degree at Qilu University of Technology. Her research is focused on bioanalytical chemistry.



Shiwei Liu was born in 1997 and received his B.S. degree from Qilu University of Technology in 2020. He is now studying for a Master degree at Qilu University of Technology. His research is focused on bioanalytical chemistry.



Quan Yuan was born in 1982 and received her PhD from Peking University in 2009. Currently, she is the Professor in Hunan University. She is the gainer of Nano Research Young Innovators Award (2018), Young Cheung Kong Scholars Program (2015), The Chinese Chemistry Society Young Chemist Award (2015), Excellent Young Scientist Foundation of NSFC (2014), Program for New Century Excellent Talents in University of Ministry of Education of China (2013). Her research interests focus on the development of designs of multifunctional nanomaterials, and biomedical applications of analytical detection and bioimaging.